Journal of Achievements in Materials and Manufacturing Engineering
VOLUME 32
ISSUE 2
February
2009

# Ferritic-austenitic steel and its weldability in large size constructions

**J. Nowacki** *
West Pomeranian University of Technology, Al. Piastów 17, 70-310 Szczecin, Poland
* Corresponding author: E-mail address: jnowacki@ps.pl

Received 06.01.2009; published in revised form 01.02.2009

Materials

## ABSTRACT

**Purpose:** On the basis of sources and own experiments, the analysis of microstructure, properties, applications as well as material and technological problems of ferritic-austenitic steel welding were carried out. It was shown the area of welding applications, particularly welding of large-size structures, on the basis of example of the FCAW method of welding of the UNS S3 1803 duplex steel in construction of chemical cargo ships.

**Design/methodology/approach:** Influence of selected aspects of welding technology, including welding heat input and between-bead temperature, additional materials on microstructure transitions and properties of welded joints were analysed. In the described work, experiments were conducted to welding tests for selected joints, visual examinations, non-destructive testing of welded joints, X-ray examinations, and metallographic testing of welded joints.

**Findings:** As a result of the performed inspection, decreasing of the ferrite content with the increase of the root face gap (increase of welding heat input) was observed. The measured ferrite content was not lower than 28 %, and the maximum value did not exceed 69% (the permissible range being from 25 to 70 %).

**Research limitations/implications:** The welding heat input exceeding the recommended values might influence the precipitation processes in the HAZ, what need further experiments.

**Practical implications:** Application of high value of the welding heat input will be profitable in terms of the welding costs.

**Originality/value:** An original value of the paper is to prove that a usage of high value welding heat input provides the best joints quality.

**Keywords:** Duplex steel; Welding; Microstructure Properties and Testing of welded joints

**Reference to this paper should be given in the following way:**
J. Nowacki, Ferritic-austenitic steel and its weldability in large size constructions, Journal of Achievements in Materials and Manufacturing Engineering 32/2 (2009) 115-141.

## 1. Introduction

Due to its chemical constitution and the ferritic-austenitic microstructure, the duplex steel concentrates the best properties of the chromium ferritic steel and chromium-nickel austenitic steel. It is characterized by very good mechanical properties: yield point, tensile strength and ductility as well as general corrosion, stress corrosion and pitting corrosion resistance.

Relatively low cost of production of the duplex steel, in comparison with the austenitic steel, is among other things caused by lowered content of expensive and scarce nickel, what is its next advantage. Improvement of steel chemical constitution in successive years, among other things as a result of increase of molybdenum and nitrogen content, increased its microstructure stability and further improvement of its properties. Use of the ferritic-austenitic steel, first of all in case of welded structures, caused particular interest with its weldability. It is commonly thought that the duplex steel belongs under the category of relatively easy weldable. However, examples of serious difficulties are known, occurring particularly during welding of construction of large dimensions, what caused considerable financial losses connected with necessity of repairs and additional inspections of welded joints [1-4].

## 2. Microstructure and properties of the duplex steel

In comparison with the austenitic steel, the ferritic-austenitic steel – duplex Cr-Ni-Mo (Table 1) contains less of expensive nickel and is characterized by considerably better mechanical properties, having at the same time good formability and corrosion resistance, also in mediums containing chloride ions. Similar proportion of high-chromium ferrite and austenite featuring by high ductility causes that the duplex steel maintains a good crack resistance in temperature up to approximately -40°C.

However, high-chromium ferrite is the metastable phase, so the temperature range of use of that steel is limited to approximately 300°C. Steel containing approximately 22% Cr, 5% Ni, 3% Mo and up to 0.2% N crystallizes as a solid solution δ, changing partially from temperature of approximately 1200° C to 850° C into the phase α. Stable steel structure in the temperature of 850° C is ferrite, while in a lower temperature - mixture of phases of γ + σ + α (Figure 1) [1].

Steel obtains the two-phase structure α + γ after supersaturating from the temperature of stability of a mixture of phases α + γ and the portion of phases depends on supersaturating conditions. Supersaturating from the temperature nearly 1200°C in water provides appearance of a high portion of high-chromium ferrite and a low portion of austenite in the steel structure. It causes increase of mechanical properties and decrease of steel plasticity as well as the crack and corrosion resistance. Lower cooling rate from the mentioned temperature, e.g. in air, allows for a partial transition α → γ and the increase of austenite portion in the steel structure, improving plastic properties. A value of the cooling rate from the temperature of the end of steel hot working or air welding does not cause the transition of the high-chromium ferrite into phases σ + γ [1]. The ferritic-austenitic steel should contain from approximately 40 to 60% of the phase γ. A portion of the phase γ beyond supersaturating conditions considerably depends on chemical constitution of steel, i.e. type and concentration of ferrite and austenite forming components.

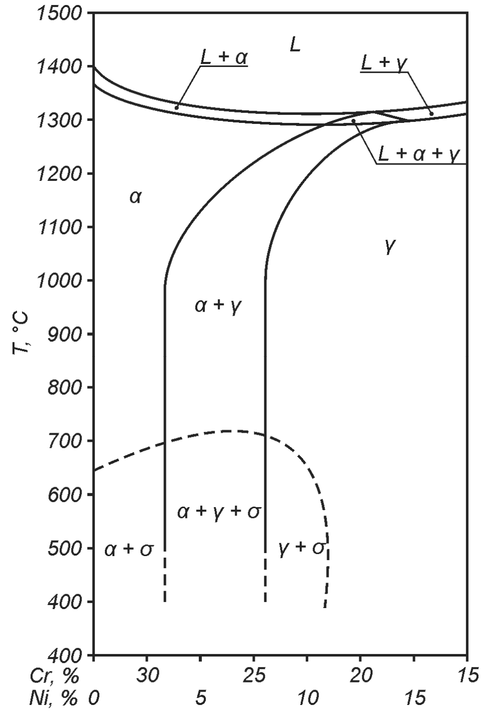


Fig. 1. Section of a phase equilibrium system of Fe-Cr-Ni alloys at concentration of 70% [6]

Nitrogen is interesting as the alloying component in the duplex type steels, allowing decrease of scarce nickel concentration, possible as a result of introduction of nitrogen into steel in the amount of over 0.2%, what requires the use of special technologies, e.g. the pressure electroslag remelting or the powder metallurgy [1].

Table 1.
Approximate chemical constitution and heat treatment conditions of the duplex steel [5]

| Steel marking | Concentration of chemical elements 1), % | | | | | | Hyperquenching temperature, °C /cooling medium 2) |
|---|---|---|---|---|---|---|---|
| | C | Cr | Ni | N | Mo | other | |
| X2CrNiN23-4 | ≤0.03 | 23 | 4.5 | 0.13 | 0.35 | Cu:0.35 | 950-1050/w,p |
| X2CrNiCuN23-4 | ≤0.03 | 23 | 4.5 | 0.13 | 0.35 | Cu:2 | 950-1050/w,p |
| X2CrNiMoSi18-5-3 | ≤0.03 | 18.5 | 4.9 | 0.08 | 2.8 | Si:1.7 | 1000-1100/w$_f$p |
| X3CrNiMoN27-5-2 | ≤0.05 | 26.5 | 5.5 | 0.13 | 1.7 | - | 1020-1100/w,p |
| X2CrNiMoN22-5-3 | ≤0.03 | 22 | 5.5 | 0.16 | 3 | - | 1020-1100/w,p |
| X2CrNiMoN29-7-2 | ≤0.03 | 29 | 6.7 | 0.35 | 2.1 | Cu≤0.8 | 1040-1120/w,p |
| X2CrNiMoCuN25-6-3 | ≤0.03 | 25 | 7 | 0.25 | 3.5 | Cu:1.8 | 1040-1120/w,p |
| X2CrNiMoN25-7-4 | ≤0.03 | 25 | 7 | 0.3 | 3.8 | - | 1040-1120/w,p |
| X2CrNiMoCuWN25-7-4 | ≤0.03 | 25 | 7 | 0.25 | 3.5 | Cu:0.8, W:0.8 | 1040-1120/w.p |

1) P≤0.03-0.035, S≤0.015, Si≤0.5-1, Mn≤1-2; values without character ≤ mean average concentration.
2) w - water, a - air.
3) According to PN-EN 10088-3:2007.

The duplex steel has a carbon concentration limited to <0.03% with the aim of decreasing the brittle fracture appearance transition temperature (FATT) of the high-chromium ferrite as well as 21 to 28% Cr, 3.5 to 8% Ni, 0.1 to 4.5% Mo, 0.05 to 0.35% N, and sometimes also 0.1 to 2.5% Cu and up to 1% W.

In the supersaturated state, steel gains good mechanical properties: $R_{0.2}$ from 400 to 530 MPa, $R_m$ from 600 to 930 MPa, elongation over 20 and > 25%, breaking energy of the Charpy V longitudinal samples $KV_{20°C}$ more than 80 as well as > 100 J and a good intercrystalline corrosion resistance also after welding. In the course of soaking in the temperature range from approximately 350 to over 500°C the phase α is subject to the spinodal transition to isomorphous areas of diversified Cr concentration, causing occurrence of embitterment 475°C. Transitory soaking of steel in the temperature over 600°C causes precipitation hardening of the phase α through dispersion particles of nitrides $Cr_2N$ and $Mo_2N$ as well as CrN and MoN, carbides $M_{23}C_6$ and the phase χ-$Fe_{36}Cr_{12}Mo_{10}$, while during long-running soaking at those conditions it takes place the complete change of ferrite into the phase χ, σ and the low-alloyed austenite [1].

The duplex steel impact resistance at the room temperature is comparable to that of the austenitic steel; however, it clearly decreases when decreasing the temperature of testing. The brittle fracture appearance transition temperature (FATT) of ferritic-austenitic steels amounts to approximately -50°C (Figures 3, 4, Table 2). Higher hardness of the duplex steel in comparison with the austenitic steel is connected with higher resistance of the two-phase structure and causes that the duplex steel features with good abrasive wear resistance erosion resistance.

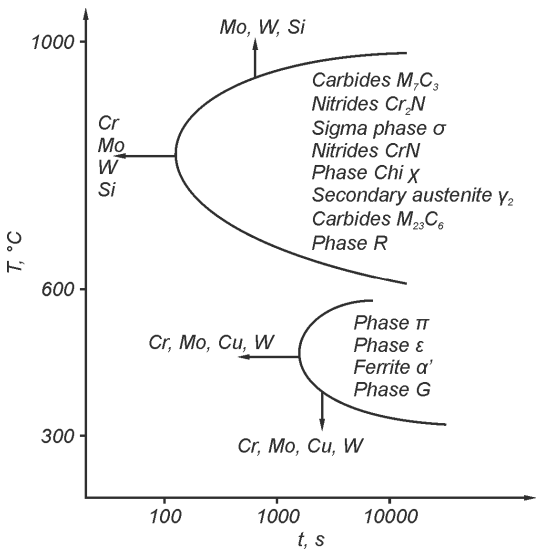


Fig. 2. Influence of alloy additions on CTP curves and precipitation processes in the ferritic - austenitic duplex steels [8]

In the temperature range of 300-1000°C, as a result of precipitation processes depended on conditions of heat treatment or thermal cycle of welding, in the duplex steels, in the groundmass of ferrite and austenite, the secondary phases differentiated in respect of the chemical constitution and structure may nucleate and grow (Figure 2) [5-9]: high-chromium ferrite α`, secondary austenite $γ_2$, phase σ (Fe-Cr-Mo) of the AB type, phase χ ($Fe_{36}Cr_{12}Mo_{10}$) of the $A_{48}B_{10}$ type, carbides $M_7C_3$ and $M_{23}C_6$, nitride of π type $M_5N$ ($Fe_7Mo_3N_4$), chromium nitrides $Cr_2N$ and CrN, phase R ($Fe_{28}Cr_{13}Mo_{12}$), phase τ (Fe, Cr, Mo, Ni), phase G, phase ε.

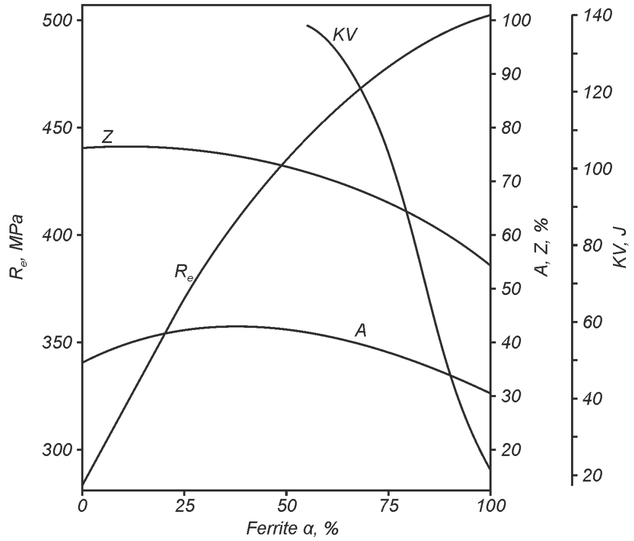


Fig. 3. Influence of ferrite relative volume on mechanical properties of the ferritic - austenitic steel containing 23% Cr, 3% Mo, 0.05% C and changeable quantity of nickel [12]

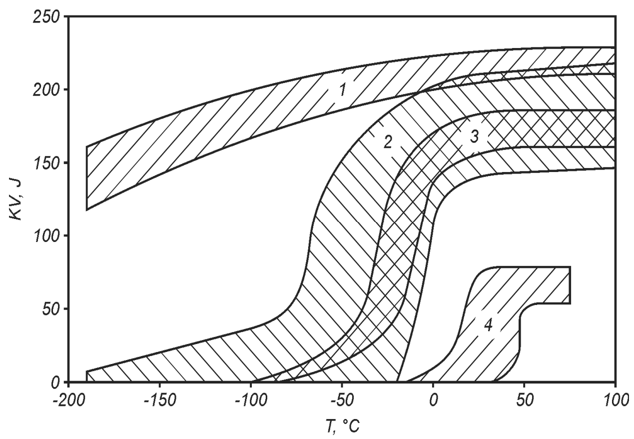


Fig. 4. Dependence of the breaking work as a function of temperature of testing the corrosion resistive steels; 1 – austenitic steel, 2 – ferritic steel, 3 – austenitic-ferrictic steel, 3 – martensitic steel [8, 13-15]

The mechanical properties and corrosion resistance of the duplex steel are determined by its microstructure, mainly the relative volume of ferrite and austenite. Increase of the austenite relative volume provides ductility and impact resistance as well as increases corrosion resistance while the increase of the ferrite relative volume increases the tensile strength; yield point and hardness of the steel. Advantageous mechanical properties of the steels are caused by their close-grained structure as well as presence of the interstitial solution of nitrogen in austenite. Nitrogen, when dissolving in austenite, causes the increase of its mechanical properties to the level of ferrite properties. The tensile strength of the duplex steel is approximately two times higher than its field point while in austenitic steel that quotient amounts to approximately 0.35. Cold working may cause the increase of the steel yield point value even to approximately 1000 MPa. In the course of using the steel at heightened temperatures, the yield point value decreases. It is caused by reduction of strengthening effect of nitrogen, atoms of which become more lively and they obstruct dislocation motion in less degree.

Addition of silicon (up to 2%) provides advantageous influence on corrosion resistance in the intensive nitric acid, and also increasing the oxidation resistance at a high temperature. There are known duplex steels containing 3.5 to 5.5% Si of raised pitting and stress corrosion resistance [10]. Tungsten of content up to 2%, stabilizing ferrite, increases steel pitting corrosion resistance, and also crevice corrosion resistance in hot chloride solutions [11].

To obtain the ferritic-austenitic structure to balance influence of ferrite forming chemical elements it is necessary to introduce to the steel the austenite stabilizing chemical elements, e.g. nickel of content 3 to 8%, which at the same time increases the passivity of the steel and corrosion resistance of the steel in mediums of organic and mineral acids.

Nitrogen allows for decreasing the content of nickel. It improves the weldability, mechanical properties and steel pitting corrosion resistance. Introduction more than 0.2% of nitrogen to steel requires the use of special technologies, e.g. powder metallurgy or pressure electroslag remelting. Content of nitrogen in the duplex steel amounts to approximately 0.15%, while of the superduplex type steels approximately 0.3%, what allows for higher solubility of nitrogen in alloys of higher content of alloying elements, particularly chromium, manganese and molybdenum increasing its solubility in austenite [17].

In the duplex steel, manganese increases abrasive and adhesion wear resistance as well as mechanical properties without decreasing the steel ductility. Manganese content in the duplex steel does not exceed 2%, as above 3% it decreases the CPT (*Critical Pitting Temperature*) as a result of creation of nuclei of pitting corrosion, what are manganese sulphides.

Copper increases the steel corrosion resistance in non-oxidizing mediums. High concentration of copper influence on worsening hot plasticity and weldability; for this reason its concentration in steel is limited to approximately 2% [18].

Low content of carbon has the essential positive influence on the duplex steel corrosion resistance. In the Cr-Ni steel the solubility of carbon in austenite at the room temperature amounts to approximately 0.04% and decreases when the temperature is decreased. Content of carbon in the duplex steel was limited to approximately 0.03% to stop release of chromium carbides, which contribute to impoverishment of areas adjacent to grain boundaries with chromium and sensitizing to intercrystalline corrosion.

Properties of the duplex steel essentially depend on segregation of alloy-forming elements in austenite and ferrite. Ferrite has more Cr, Si, Mo, W and P, while austenite – Mn, Cu, Ni and N. The proper content of alloy-forming elements in steel, mainly Cr, Mo and Ni, provides obtaining a stable passive state of steel in the air and aggressive corroding mediums (Figure 5, Tables 3, 4).

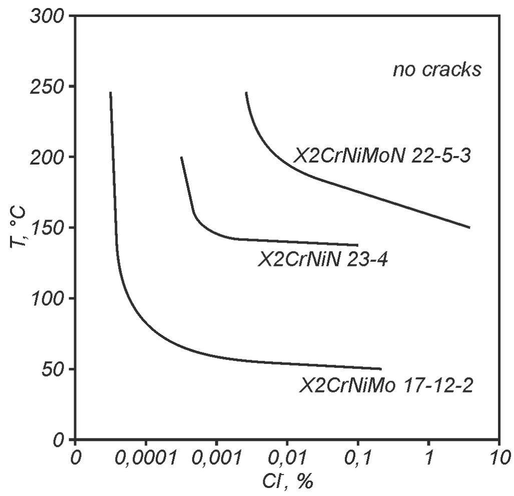


Fig. 5. Stress corrodibility as a function of temperature and concentration of $Cl^-$ ions; tests at the steady load amounting to the yield point, test time 1000 h [19]

To determine the pitting corrosion resistance of the discussed steels the PRE (*Pitting Resistance Equivalent*) is used:

$$PRE_N = \% Cr + 3.3\% Mo + 16\% N \quad (1)$$

In steels containing tungsten additions, the PRE equivalent is calculated in accordance with:

$$PRE_W = \% Cr + 3.3(\% Mo + 0.5 \% W) + 16\% N \quad (2)$$

Alloys of the PRE equivalent value higher than 40 are included among those particularly pitting corrosion resistant and are used in very aggressive environments, e.g. in sea water, in the medium of dilute hydrochloric and sulphuric acid. Another method of estimation of steel susceptibility to that type of corrosion is the CTP (Critical Pitting Temperature) determining the lower temperature in which pitting corrosion in the $FeCl_3$ solution will appear at changeable temperature of testing.

High intercrystalline resistance of the duplex steel is connected with its resistance to sensitization and high value of the diffusion coefficient in ferrite, 100 times higher than that in austenite, allowing for homogenizing of the chromium content in the interior and grain boundary areas. The ferritic - austenitic steel is more resistant to intercristalline corrosive effect than the austenitic steel of the same carbon content. The ferritic - austenitic steel is more resistant to intercrystalline corrosion in comparison with the austenitic steel of the same carbon content, while for carbon content less than 0.02% may be completely resistant for that type of corrosion.

Corrosion resistance of the dual phase duplex steel in organic acids is comparable with the resistance of the high-chromium austenitic steels. Corrosion resistance of the duplex steel in the acids of reducing properties depends on the susceptibility to steel passivity, while in the acids of oxidizing properties on the corrosion resistance of the surface layer. A good resistance to the impact of organic acids also characterizes the duplex steel.

Table 2.
Mechanical properties in the room temperature of the duplex steel in the supersaturated state and the ferritic steel in the annealed state [16]

| Steel marking | Yield strength $R_{e0.2}$, MPa | Tensile strength $R_m$, MPa | Elongation A, % | Breaking energy, J | Hardness, HB |
|---|---|---|---|---|---|
| X2CrNiN23–4 | 400-420 | 620-830 | 20 | 100 | 260 |
| X2CrNiMoN22–5–3 | 460-480 | 650-880 | 25 | 100 | 270 |
| X2CrNiMoCuN25–6-3 | 490-510 | 700-900 | 25 | 100 | 270 |
| X2CrNiMoN25–7–4 | 530-550 | 730-930 | 25 | 100 | 290 |
| X2CrNiMoCuWN25–7–4 | 550 | 730-930 | 25 | 100 | 290 |

Table 3.
Comparison of the stress corrosion resistance of austenitic steel and the duplex steel [13]

| Steel marking | Corrosive medium | | | | | | | |
|---|---|---|---|---|---|---|---|---|
| | 42% $MgCl_2$ 154°C | 35% $MgCl_2$ 125°C | Drop evaporation 0.1M NaCl 120°C | Wick's test 1500 ppm Cl in NaCl 100°C | 33% $LiCl_2$ 120°C | 40% $CaCl_2$ 100°C | 25-28% NaCl 155°C | 26% NaCl 200°C |
| Austenitic steel | | | | | | | | |
| X2CrNiMo17-12-2 | - | - | - | - | - | - | - | - |
| Ferritic-austenitic steel | | | | | | | | |
| X2CrNiN23-4 | - | - | - | - | + | + | + | - |
| X3CrNiMoN22-5-3 | - | - | - | + | + | + | + | - |
| X2CrNiMoN25-7-4 | - | - | - | + | + | + | + | - |
| X2CrNiMoCuWN25-7-4 | - | - | - | + | + | + | + | - |

- probability of cracking, + no cracks

Table 4.
Denotations, chemical constitution and PRE equivalent of the duplex steel [12, 20]

| Steel marking | Commercial denotation | Content of alloy additions, %[5)] | | | | | | $PRE_N$ | $PRE_W$ |
|---|---|---|---|---|---|---|---|---|---|
| | | C | Cr | Ni | Mo | N | other | | |
| X2CrNiN23-4 | SAF 2304[1)] UR 35 N[2)] | ≤0.03 | 23 | 4 | 0.2 | 0.1 | Cu: 0.35 | 24 | |
| X3CrNiMoN22-5-3 | UR 45 N[2)] SAF 2205[1)] UR 45 N+[2)] | ≤0.05 | 22 | 5 | 2.8 | 0.15 | - | 32/33 | |
| | | ≤0.03 | 22.8 | 6 | 3.3 | 0.18 | - | 35/36 | |
| X2CrNiMoCuN25-6-3 | UR 52 N[2)] | ≤0.03 | 25 | 6.5 | 3 | 0.22 | Cu: 1.5 | 38/39 | |
| | UR 47 N[2)] | | 25 | 6.5 | 3 | 0.22 | | 38/39 | |
| | DP 3[3)] | | 27 | 7 | 3 | 0.16 | Cu: 0.5 W: 0.3 | 37 | 38 |
| X2CrNiMoCuN25-6-3 | UR 52 N+[2)] | ≤0.03 | 25 | 7 | 3.5 | 0.25 | Cu: 1.5 | 41 | |
| X2CrNiMoN25-7-4 | SAF 2507[1)] | | 25 | 7 | 3.8 | 0.28 | - | 41 | |
| X2CrNiMoCuWN25-7-4 | Zeron 100[4)] | | 25 | 7 | 3.5 | 0.24 | Cu: 0.7 W: 0.7 | 40 | 41.5 |
| | DTS 25.7 NW[3)] | | 27 | 7.5 | 3.8 | 0.27 | Cu: 0.7 W: 0.7 | 44 | 45 |
| | DTS 25.7 NW Cu[3)] | | 25 | 7.5 | 4 | 0.27 | Cu: 1.7 W: 0.7 | 42.5 | 44 |

Producer [1)] Avesta Sheffield Ltd, [2)] Creusot-Loire Industrie, [3)] Sumitomo Metal Industries, [4)] Weir Materials Ltd,
[5)] P≤0.035; S≤0.015 - 0.03; Si ≤0.7 - 1; Mn ≤1 - 2

## 3. Application of the duplex steel

The duplex steel is the most frequently used after annealing at the temperature of 1020 to 1100°C and cooling in water, providing portion of approximately 50% ferrite and 50% austenite in the structure. The portion of the duplex steels in the use of alloy steels amounts to approximately 1%, but demand for that steel continuously increases.

The corrosion-resistant ferritic-austenitic steel is an attractive alternative for the standard single-phase austenitic and ferritic steel [20, 21]. Advantages and weaknesses decide on the area of application of the duplex steel.

Main advantages of the duplex steel include:

- moderate price in comparison with the high - nickel steel,
- high yield point, almost two times higher than the yield point of the austenite steel,
- low coefficient of thermal expansion,

high corrosion resistance, resulting mainly from high content of the alloying elements: Cr, Mo, N.

The main weakness of the duplex steel is limitation the temperature of its use to approximately 250-300°C and the increase of its brittleness as a result of a long-lasting influence of an elevated temperature causing brittleness 475°C [21].

The modern duplex steel features in very good mechanical properties in the temperature range from approximately -50°C to 250°C and a good weldability. It is characterized by the high pitting corrosion resistance, stress corrosion resistance and in many corroding mediums it has better properties than the austenitic steel containing comparable quantities of Cr and Mo additions. It is used to build structures and facilities operated in seawater as well as in the atmosphere contaminated with hydrogen sulphide and other chemically aggressive substances, structures and facilities in the extractive industry of crude oil and gas, in building the chemical cargo carriers as well in the papermaking, chemical and food industry [1].

The main examples of application of the duplex steel are:

- elements of heat exchangers (light-wall tubes and heavy wall tubes for gas and oil),
- elements of pipelines of desalination systems,
- elements of pressure vessels (tubes, systems for technological processing and transportation of chemicals),
- pipelines in the processing industry for transportation of solutions containing chlorides,
- rotors, fans, shafts and press rollers, which should have the high corrosion fatigue strength,
- tanks and pipelines in the shipbuilding industry, in chemical cargo carriers,
- offshore systems,
- parts of machines and facilities in the papermaking industry,
- the extractive industry of crude oil and gas, installations on oil fields and for transportation of crude oil,
- tanks and systems in the petrochemical industry.

The duplex steel is also used in the Polish chemical industry, e.g. in structures of heat exchangers, where the duplex steel was used as an anticorrosive coating padded on the low-alloy steel to protect it against corrodible effect of the ammonium urethane. One of the most important areas of applications of the duplex steel is the shipbuilding industry, where it is used in structures of chemical cargo carriers. In 1970 in the Dunkerque Shipyard the first chemical cargo carrier was built using the duplex steel.

Welding technique of the duplex steel in large-size structures products a lot of problems, so few shipyards all over the world undertake the risk of production the chemical cargo carriers of that steel [22]. Chemical cargo carriers are accommodated to transportation of chemical cargo as well as products of crude oil refining, acids, vegetable oils, animal fats, wine and molasses. Additionally they are accommodated to transportation of such freights as e.g. hexamethylenedimene, n - pentane, i – pentane, naphthalene, phosphoric acid. Structure of the hull of a ship takes into consideration the condition of internal stresses and external loads, type and arrangement of the transported cargo as well as operating needs: among other things, simultaneous transportation of different chemical individuals in separate load tanks as well as requirements of regulations of classification societies and operating conditions.

In case of chemical cargo carriers of lower displacement (below 40 000 DWT) the cargo space is divided into separate parts, where wing tanks from the left and right ship’s side and the central tanks may be distinguished. The longitudinal tanks are divided with longitudinal corrugated bulkheads of vertical waves. The external tanks are enclosed with a double bottom, double side bulkheads and the upper deck.

Division into smaller tanks is made by means of corrugate bulkheads of the horizontal or vertical wave arrangement [22]. Due to lower carrying capacity, lower external loads and internal stresses, design of corrugated bulkheads fully ensures rigidity of the hull internal structure, and all backstays are installed outside the cargo tanks (i.e. in the double bottom, side bulkheads and on the upper deck).

In case of ships of higher displacement (above 40 000 DWT) the design of the hull of a ship is somewhat different. A cargo tank area of the chemical cargo carriers has a separated central section and side sections, divided by means of longitudinal flat bulkheads of the cofferdam type [22]. The central section is divided into tanks, including liquid waste tanks. The side sections are also divided into tanks. Division into the tanks is made by means of corrugated bulkheads (Figure 6).

Thickness of duplex steel sheets used for structures of cargo tanks in the chemical cargo carriers is situated in the range from 8.5 to 32 mm and is usually differentiated in individual areas of structure of the tanks [22].

All cargo tanks made of the duplex steel in chemical cargo carriers have internal surface free of structural components. In the structure of tank shells of ships all joints, both butt joints and tee joints, are made as groove welds of thorough penetration, forming homogeneous joints of the duplex steel. Remaining structural components in joints with elements of tanks of the duplex steel create mixed connections with the carbon steel or higher-strength steel. The mixed connections in butt joints are made as groove welds of thorough penetration while tee joints are mainly formed with fillet welds.

Presence of structural components from the side of external surfaces of the tanks causes the necessity of making mixed connections and homogeneous on high number of sealing elements of small sizes, which form both lap joints welded with fillet welds and tee joints welded, depending on type of the node, with fillet welds or groove welds of thorough penetration.

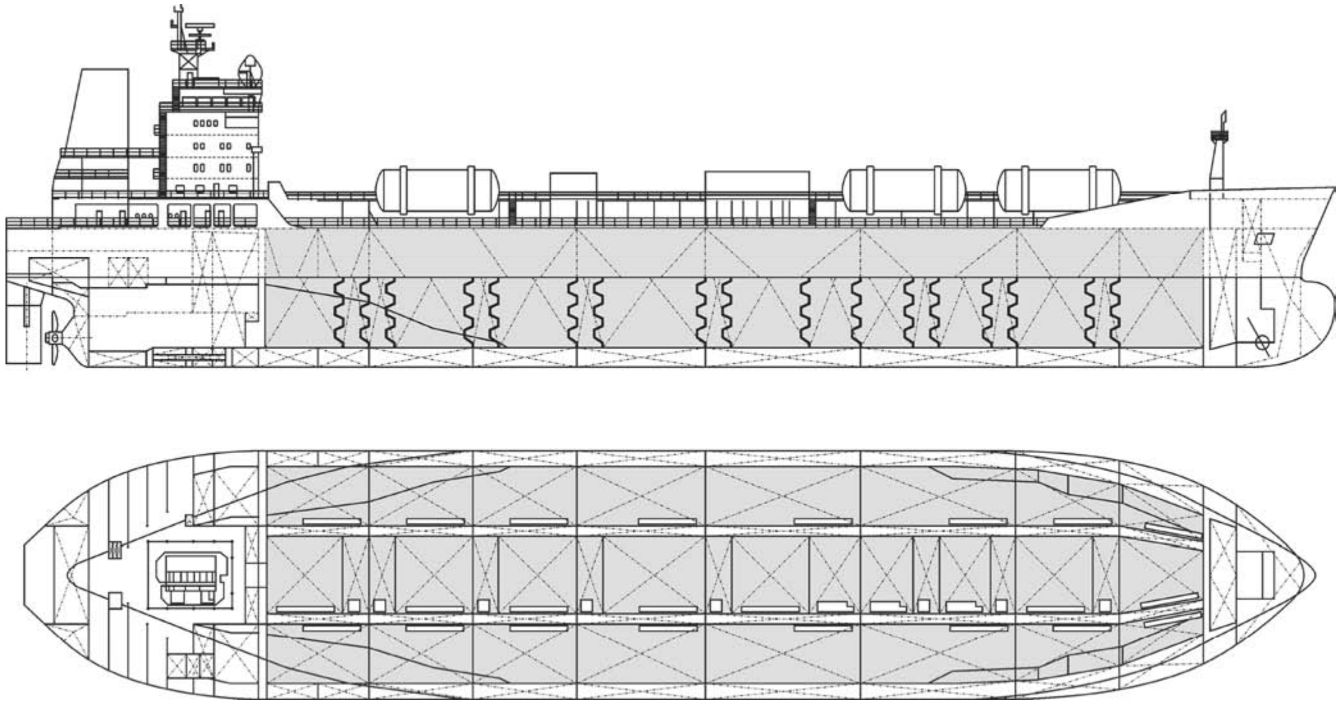

Fig. 6. An example of arrangement of cargo tanks made of the austenitic-ferritic steel in a modern chemical cargo carrier; the space where there are the cargo tanks are distinguished with the grey colour, according to [22]

The mentioned types of welded and mixed joints cause the demand for execution of welding work of the total length of approximately 48.000 m per ship, including butt joints with groove welds (approximately 10.000 m), tee joints with groove welds (approximately 8.000 m), fillet welds in the tee and lap joints (approximately 30.000 m).

## 4. Local weldability of the duplex steel

Phase transitions in the duplex steel during heating and cooling exert considerable influence on the structure, phase composition and phase morphology as well as mechanical properties of a welded joint. Use of additional welding materials of a composition similar to steel composition causes that the joint immediately after solidification has a structure of the solid solution $\alpha$, which during cooling undergoes a partial transition into austenite (Figure 7). Portion of the phase $\gamma$ and its morphology depend on a cooling rate of the joints in the range of the phase $\alpha$ stability, i.e. up to approximately 850°C. It also concerns a fused zone as well as a heat affected zone heated to the temperature exceeded the transition line $\alpha + \gamma/\alpha$ [1].

The welding heat input, size of jointed elements as well as the value of between-bead temperature exerts a considerable influence on a width of the heat affected zone, relative volume, size and morphology of grains of phases $\alpha$ and $\gamma$. A high value of welding heat input causes increasing a width of the heat affected zone and growth of grains of the phase $\alpha$ and decreasing a cooling rate of a welded joint as well as the increase of a relative volume of the phase $\gamma$. Austenite forming in a heat affected zone, marked sometimes as $\gamma_2$, contains less Cr and more Ni in comparison with the phase $\gamma$ appearing in steel. At a low value of the welding heat input, a cooling rate of joints is high as a result of intensive heat abstraction through jointed elements of a high thermal capacity. Then only a small part of the phase $\alpha$ changes into the phase $\gamma$ and a joint structure has morphology similar to morphology of the Widmanstaten structure. A cycle of phase transitions taking place during heating in the joints welding and cooling process happens again during building up a successive weld layer. Differentiated cooling conditions after building up the successive weld layers caused a different portion of the phases $\alpha$ and $\gamma$ as well as their morphology in a face and root of a welded joint [1]. A cooling rate of the welded joint from the temperature of stability of the phase $\alpha$, i.e. approximately 850°C should be high enough to not allow for arising of release processes and transitions of the high-chromium ferrite into phases $\sigma$, $\chi$ and similar to them as to structure and the low-alloyed austenite, as it causes the decrease of ductility and corrosion resistance of the welded joint. Hence, it also results the necessity of limitation a between-bead temperature to < 200°C [1].

Short impact times of high temperatures and high temperature gradients in a heat affected zone decide on the specificity of release processes as well as transitions the ferrite into the austenite $\gamma$ and secondary austenite $\gamma_2$. Depending on a temperature what will be gained in a heat affected zone in the course of carrying out a successive bead, there are formed conditions of nucleation and growth of carbides ($M_{23}C_6$, $M_7C_3$), nitrides ($CrN$, $Cr_2N$) and austenite ($\gamma_2$), very differentiated in respect of the chemical constitution, structure and types of releases of intermetallic phases ($\sigma$, $\chi$, R, G, $\pi$, $\tau$).

a)

b)

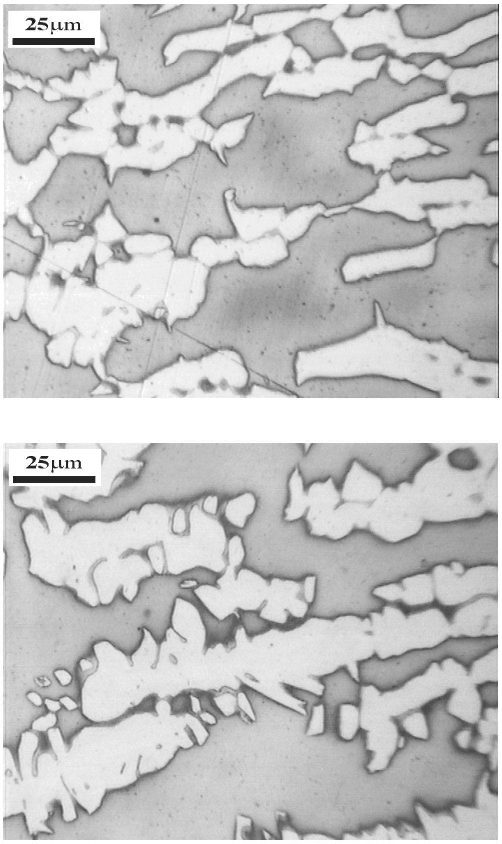


Fig. 7. Microstructure of a heat affected zone, ferrite – dark phase, primary austenite – light phase, welding heat input: a - 1.6 kJ/mm, relative volume of ferrite - 54%, b - 2.2 kJ/mm, relative volume of ferrite - 48%, [24]

As a result of cooling from temperatures above the transition line $\alpha \rightarrow \alpha + \gamma$, in the thermodynamic equilibrium system Fe-Cr-Ni, the primary austenite $\gamma$ is formed as a product of the transition $\alpha \rightarrow \gamma$. The secondary austenite $\gamma_2$, fundamentally differing with the composition, morphology and properties from the primary one, is formed in the duplex steel as a result of the transition $\alpha + \gamma \rightarrow \alpha + \gamma + \gamma_2$ in the austenitic-ferritic structure after its heating to the temperature below the transition line $\alpha \rightarrow \alpha + \gamma$ in the thermodynamic equilibrium system Fe-Cr-Ni.

Mechanical properties and a corrosion resistance of a heat affected zone of the duplex steel depend on the relative volume of ferrite and austenite, morphology and grain size of ferrite and austenite as well as the type, morphology and distribution of carbides, nitrides and a series of intermetallic phases, influence of which on properties of a heat affected zone is the most frequently disadvantageous. The width of a heat-affected zone depends first of all on the quantity of a welding heat input as well as a section of the joint welded. When welding at a small welding heat input, the growth of ferrite grains as well as intensity of the transition $\alpha \rightarrow \gamma$ is limited. In case of high concentration of austenite-forming chemical elements (Ni, Mn, Cu, N, C) and a large heating rate, the transition point $\gamma \rightarrow \alpha$ may increase to such a level that the growth of ferrite grains will be also limited [23].

## 5. Duplex steel welding techniques

Arc welding of the duplex steel is possible, depending on conditions and volume of production, using the following methods:

- shielded manual arc welding (SMAW),
- non-consuming electrode gas-shielded welding (GTA),
- consumable electrode active gas-shielded welding (GMAW)
- flux-cored arc welding (FCAW),
- submerged arc welding (SAW),
- plasma-arc welding (PAW).

In large factories of a differentiated production range, the arc welding process is the most frequently carried out using the following methods [22]:

- 121 ( SAW ) – submerged arc welding,
- 111 ( SMAW ) – with a shielded electrode,
- 136 ( FCAW ) – with a flux-cored wire.

## 6. Parent and additional materials

The most frequently used parent material is the UNS 31803 steel (X2CrNiMo 22-5-3) (≤0.03% C; 21-23% Cr; 4.5–6.5% Ni; 2.75-3.5% Mo; ≤2.0% Mn; ≤1.0% Si; 0.15-0.19% N; ≤0.03% P; ≤0.02% S) welded with the flux-cored wire method FCAW as one of the most developmental arc welding method of the duplex steel, having the largest portion in consumption of deposited metal. Welding with flux-core wires with the FCAW methods makes the largest portion in execution of building the chemical cargo carriers. Welding on ceramic straps is used in a significant degree [22]. In case of tee joints and butt joints of the thickness value more than 17 mm, round washers of a diameter depended on the threshold spacing (usually 10 or 12 mm) is most frequently used. Two-operator welding is used. In butt joints of sheet thickness below 17 mm it is used the method of one-operator welding using banking straps. A range of application of the FCAW method when welding field joints (corrugated, cofferdam bulkheads and the inner bottom) of chemical cargo carriers built in SSN is shown in Figures 8 and 9.

To obtain the proper structure of a joint welded, mechanical properties and corrosion resistance, flux-cored wires used for welding of the duplex steel must contain higher quantity of alloy-forming elements (first of all Cr, Ni, N) in comparison with the basic material. Ni and N, as chemical elements stabilizing the austenite structure, ensure obtaining the suitable portion of that phase in the joint structure.

At present, a dozen or so types of flux-cored wires are manufactured (Tables 5, 6).

Chemically active gases or gas mixtures are used for welding of the duplex steel (Tables 7, 8). In case of use the pure $CO_2$ as a shield of the electric arc of a flux-cored wire, it appears the wider surface of introduction of arc heat to the welding puddle in comparison with mixtures basing on Ar. It takes place due to the higher thermal conductivity of pure $CO_2$, what in turn provides the advantageous, circular shape of a weld penetration line, higher than that of the $Ar+CO_2$ mixtures (particularly when using better parameters of welding).

Fig. 8. A section of the tank welded using the FCAW method during assembling on a slipway [22]

It influences on lower risk of appearance of incomplete fusions and entrapped slums in a joint welded. Pure $CO_2$ destabilizes electric arc burning, so to ensure the spraying metal transfer, a suitable fusing agent composition is used as well as deoxidizers, which reduce an oxidizing effect to metal of a welding puddle.

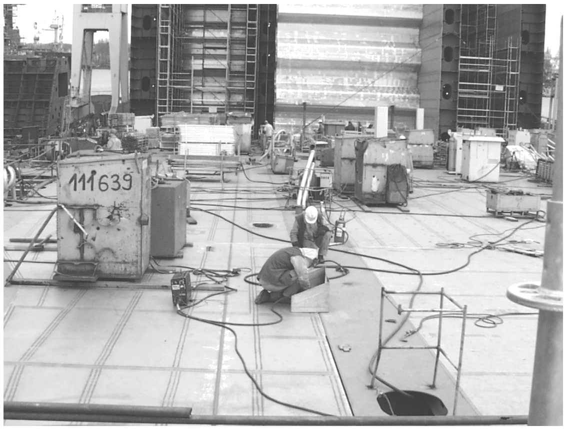

Fig. 9. A section of the inner bottom welded using the FCAW method during assembling on a slipway [22]

Table 5.
Chemical constitution of a deposited metal of selected flux-cored wires [22]

| Producer/ Marking | Classification according to AWS A5.22 | Chemical constitution, % mass fraction | | | | | | | | | | | |
|---|---|---|---|---|---|---|---|---|---|---|---|---|---|
| | | C | Cr | Ni | Mo | Si | Mn | N | V | Nb | Cu | P | S |
| Elga/Cromacore DW 329A | E2209T0-4/-1 | 0.02 | 22.9 | 9.2 | 3.0 | 0.8 | 1.3 | 0.10 | 0.1 | 0.08 | 0.02 | 0.020 | 0.007 |
| Elga/Cromacore DW 329AP | E2209T1-4/-1 | 0.02 | 22.9 | 9.2 | 3.0 | 0.8 | 1.3 | 0.10 | 0.1 | 0.08 | 0.02 | 0.020 | 0.007 |
| Esab/OK Tubrod 14.27 | E2209T1-4/-1 | <0.04 | 22.0 | 9.0 | 3.0 | 0.85 | 0.9 | 0.11 | dnt | dnt | dnt | ≤0.025 | ≤0.025 |
| Esab/OK Tubrod 14.37 | E2209T0-1 | 0.03 | 22.6 | 9.0 | 3.1 | 0.8 | 1.0 | 0.13 | dnt | dnt | dnt | ≤0.035 | ≤0.025 |
| NST/ duplex 329 J3L | E2209T1-4 | 0.028 | 22.8 | 8.84 | 2.97 | 0.39 | 1.22 | 0.12 | dnt | dnt | 0.04 | 0.018 | 0.008 |
| Avesta Welding/ FCW-2D 2205 | E2209T0-4/-1 | 0.025 | 23.3 | 9.2 | 3.3 | 0.6 | 0.8 | 0.14 | dnt | dnt | dnt | dnt | dnt |
| Avesta Welding/ FCW 2205-PW | E2209T1-4 | 0.03 | 23.0 | 9.5 | 3.5 | 0.6 | 0.8 | 0.16 | dnt | dnt | dnt | dnt | dnt |
| SAF/ Lexal T22093N | bd | 0.03 | 22.5 | 8.5 | 2.8 | 0.5 | 1.1 | 0.14 | dnt | dnt | dnt | ≤0.03 | ≤0.03 |
| SAF/Lexal TA22093N | bd | 0.03 | 22.5 | 8.5 | 2.8 | 0.6 | 0.8 | 0.14 | dnt | dnt | dnt | ≤0.03 | ≤0.03 |
| Lincoln Electric/ Cor-A-Rosta 4462 | E2209T0-4 | 0.03 | 22.9 | 9.3 | 3.4 | 0.6 | 0.9 | 0.14 | dnt | dnt | dnt | dnt | dnt |
| Lincoln Electric/ Cor-A-Rosta P4462 | E2209T1-4 | 0.03 | 22.9 | 9.2 | 3.4 | 0.6 | 0.7 | 0.14 | dnt | dnt | dnt | dnt | dnt |
| NSW/ Nittetsu SF-329J3LP | E2209T1-4 | 0.033 | 24.1 | 9.41 | 3.53 | 0.44 | 1.88 | 0.16 | dnt | dnt | dnt | 0.023 | 0.004 |
| Bohler/ CN 2209 N-FD | E2209T0-4/-1 | 0.03 | 22.7 | 9.0 | 3.2 | 0.7 | 1.1 | 0.13 | dnt | dnt | dnt | dnt | dnt |
| Bohler/ CN 2209 PW-FD | E2209T1-1/-4 | 0.03 | 22.7 | 9.0 | 3.2 | 0.7 | 1.0 | 0.13 | dnt | dnt | dnt | dnt | dnt |

dnt- data not available

Table 6.
Properties of a deposited metal of flux-cored wires for welding the duplex steel [22]

| Producer/ Marking | Shielding gas | Ferrite content | Properties | | | | | |
|---|---|---|---|---|---|---|---|---|
| | | | $R_{e0.2}$ $N/mm^2$ | $R_m$ $N/mm^2$ | $A_5$ % | KVC J | CPT °C | $PRE_N$* |
| Elga/Cromacore DW 329A | M21 (80%Ar+20%CO2) | FN40 | 610 | 800 | 32 | 40 (-20°C) | 30 | 35 |
| Elga/Cromacore DW 329AP | M21 (80%Ar+20%CO2) | FN40 | 610 | 800 | 32 | 42 (-46°C) | 30 | 35 |
| Esab/ OK Tubrod 14.27 | M21 | bd | min. 500 | min. 690 | min. 20 | 47 (-20°C) | dnt | dnt |
| Esab/ OK Tubrod 14.37 | M21 | bd | 633 | 768 | 31 | bd | dnt | dnt |
| NST/duplex 329 J3L | M21 | FN50 | 633 | 792 | 29.5 | 42 (-20°C) | dnt | 34.4 |
| Avesta Welding/ FCW-2D 2205 | M21 | FN50 | 630 | 820 | 25 | 44 (-20°C) | dnt | dnt |
| Avesta Welding/ FCW 2205-PW | M21 (80%Ar+20%CO2) | FN45 | 610 | 840 | 28 | 60 (+20°C) | dnt | dnt |
| SAF/ Lexal T22093N | M21 (82%Ar+18%CO2) | WRC92 39 | 585 | 700 | 28 | 50 (-20°C) | dnt | >35 |
| SAF/ Lexal TA22093N | M21 (82%Ar+18%CO2) | WRC92 39 | 580 | 700 | 28 | 50 (-20°C) | dnt | >35 |
| Lincoln Electric/ Cor-A-Rosta 4462 | M21 | FN40 | 665 | 825 | 29 | 38 (-20°C) | dnt | dnt |
| Lincoln Electric/ Cor-A-Rosta P4462 | M21 | FN40 | 660 | 830 | 29 | 40 (-20°C) | dnt | dnt |
| NSW/ Nittetsu SF-329J3LP | C1 (100%$CO_2$) | FN30-43 | bd | 763 | 27.6 | 40 (-20°C) | dnt | dnt |
| Bohler/ CN 2209 N-FD | M21 | FN30-50 | 600 | 800 | 27 | 40 (-40°C) | 22 | ≥35 |
| Bohler/ CN 2209 PW-FD | M21 | bd | 600 | 800 | 27 | ≥32 (-46°C) | 22 | ≥35 |

dnt- data not available
*PREN: Pitting Resistance Equivalent Number; PREN = 3.3 Cr [%] + Mo [%] + 16 N [%]

Table 7.
Shielding gases used in the welding process of the UNS S31803 steel using the FCAW method [22]

| Producer | Marking | Recommended shielding gas |
|---|---|---|
| Lincoln | Cor-A-Rosta 4462 | M21 → Ar+(5÷25%$CO_2$) |
| Lincoln | Cor-A-Rosta P4462 | M21 → Ar+(5÷25%$CO_2$) |
| Elga | Cromacore DW329A | M21 → 80%Ar+20%$CO_2$ lub C1 → 100% $CO_2$ |
| Elga | Cromacore DW329AP | M21 → 80%Ar+20%$CO_2$ lub C1 → 100% $CO_2$ |
| Esab | OK Tubrod 14.27 | M21 → Ar+(5÷25%$CO_2$) lub C1 → 100% $CO_2$ |
| Avesta Welding | 2205 FCW-2D | M21 → Ar+(15÷25%$CO_2$) lub C1 → 100% $CO_2$ |
| Avesta Welding | 2205-PW | M21 → Ar+(15÷25%$CO_2$) lub C1 → 100% $CO_2$ |
| SAF | LEXAL TA 22 9 3 N | M21 → Ar+(5÷25%$CO_2$) |
| SAF | LEXAL T 22 9 3 N | M21 → Ar+(5÷25%$CO_2$) lub C1 → 100% $CO_2$ |
| NST | NST Duplex 329J3L | M21 → Ar+(15÷25%$CO_2$) |

Table 8.
Shielding gases recommended in the welding process of the UNS S31803 steel using the FCAW method [22]

| Producer of shielding gas | Marking of shielding gas | Chemical constitution of shielding gas |
|---|---|---|
| Linde Gaz | Mison® 18 | Ar + 18%$CO_2$ + 0.03%NO |
| Linde Gaz | Mison® 25 | Ar + 25%$CO_2$ + 0.03%NO |
| Linde Gaz | Corgon® 18 | Ar + 18%$CO_2$ |
| Linde Gaz | Corgon® 25 | Ar + 25%$CO_2$ |
| BOC gazy | Argomiks C-18 | Ar + 18%$CO_2$ |
| BOC gazy | Argomiks C-20 | Ar + 20%$CO_2$ |
| Messer | FERROMIX C 18 | Ar + 18%$CO_2$ |

The shielding gas flow rate should lie within the range of 20-25 l/min. The performed tests of influence of a gas shield on geometrical and structural parameters of pudding welds carried out with flux-cored wires on the duplex steels allowed to find that geometrical properties of majority of pudding welds had been better when using $CO_2$ as a shielding gas while the M21 (Ar+25%$CO_2$) gas mixture ensured more advantageous ferrite content.

## 7. Welding heat input and between-bead temperature

The range of the recommended welding heat input should be from 0.5 to 2.5 KJ/mm. The recommended HI values and between-bead temperature when welding different grades of the duplex steel are shown in Table 9.

Table 9.
Values of HI and a between-bead temperature during welding of the duplex steel [22]

| Grade of steel | Welding heat input, HI [1] kJ/mm | Max. between-bead temperature ° C |
|---|---|---|
| 22% Cr – standard duplex steel | 0.5-2.5 | 125-200 [2] |
| 23% Cr – duplex steel without molybdenum | 0.5-2.5 | 150-200 |
| 25% Cr – duplex steel, up to 2.5% Cu | 0.2-1.5 | 100-150 [2] |

[1] HI should be selected property to the material thickness,
[2] Temperature being selected depending on the material thickness

The value of an allowable range of l welding heat input should in each case subject to verification on the basis of tests, which shall give an answer whether a technology designed for the particular grade of steel of the particular producer, accepted joint geometry, range of wall thickness, welding position, anticipated welding materials and expected joint thickness as well as values of loading them with assembly stresses meet criteria of site acceptance tests of the investor (the mechanical properties, microstructural parameters, level of corrosion resistance as well as weld quality, determined by the required level of welding incompatibilities according to non-destructive testing [22].

## 8. Welding imperfections of submerged arc welded duplex steel joints in aspects of the welding heat input

Submerged arc welding of steels demanding limited heat input of welding, e.g. high-strength steels, austenitic steels, austenitic-ferritic steels require such selection of parameters, which are a compromise between welding efficiency and joint quality [2]. Basic parameters of submerged arc welding are: arc current kind, intensity, and voltage, speed of welding, wire diameter, length of wire extension, thickness and width of welding flux layer and inclination angle of an electrode or a welded joint. Edge preparation has essential influence on quality of welding (Fig. 10).

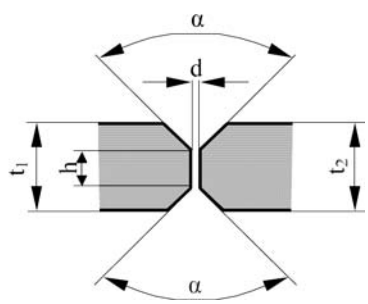


Fig. 10. Scheme of a joint preparation of submerged arc welding according to weld materials producer recommendations; width of a root face - h = 3 - 8 mm, groove angle - α = 60 - 100 °, root face gap - d = 0 - 0,5 mm, total thickness of plates - $t_1$, $t_2$ mm [2]

In the first stage of tests of duplex steel submerged arc welding, an analysis of the filler metal consumption in different variants of welding has been done with usage of the guidelines presented in literature [2] and of the recommendations of the filler metals suppliers. On account of mechanical properties and corrosion resistance, of welds main limitation of welding process of duplex steel is quantity of welding heat input - HI [2]. Plates subjected to welding are prepared according to Fig. 1, with α = 80°, h = 6 mm, d = 0-0.5 mm, $t_1 = t_2 + (2\text{-}3)$ mm, using two limits of the welding heat input: up to 2.5 kJ/mm, and up to 3 kJ/mm. Duplex steel UNS S31803 was used as a parent material. Welding of the test plates was carried out with the usage Avesta welding parent materials: wire ø 3.2 mm grade 2205, and a flux material -

Flux 805 – with alkalinity ~1.7 [2]. The welding heat input was calculated according to the Equation (1).

$$HI[kJ/mm] = \eta * \frac{I[A]*U[V]}{Vsp[mm/s]*1000} \quad (1)$$

where: HI – welding heat input, η – coefficient of welding efficiency, I – welding current intensity, U – welding voltage, Vsp- speed of welding.

Chemical composition and mechanical properties of the parent material - steel UNS S31803 and the additional materials - combination of welding wire 2205/flux 805 used in the experiment are presented in Tables 10 and 11. Welding processes have been made with the max welding heat input: HI ≤ 2.5; HI ≤ 3.0; HI ≤ 3.5; HI ≤ 4.0.

Table 10.
Results of the test of chemical composition and mechanical properties of the parent material - steel UNS S31803 used in the experiment [1]

| Chemical composition of the steel UNS S31803, average values [%] | | | | | | | | | |
|---|---|---|---|---|---|---|---|---|---|
| C | Si | Mn | P | S | Cr | Ni | Mo | N | PREN* |
| 0.03 | 0.9 | 1.8 | 0.025 | 0.015 | 22.1 | 5.2 | 2.9 | 0.17 | ≥ 34 |
| Mechanical properties, average values | | | | | | | | | |
| Re $N/mm^2$ | | | Rm $N/mm^2$ | | | KV -20°C J | | | |
| 590 | | | 780 | | | 170 | | | |

*PREN: Pitting Resistance Equivalent Number; PREN = 3.3 Cr [%] + Mo [%] + 16 N [%]; PREN minimal value, required according to international standards for planned constructions of chemical cargo ships is 34.

Table 11.
Chemical composition and mechanical properties of the additional materials - combination welding wire2205/flux 805 used in the experiment

| Chemical composition, average values [%] | | | | | |
|---|---|---|---|---|---|
| C | Si | Mn | Cr | Ni | Mo |
| 0.02 | 0.6 | 1.1 | 23.0 | 8.5 | 3.0 |
| Mechanical properties, average values | | | | | |
| Re $N/mm^2$ | Rm $N/mm^2$ | A5 % | KV +20°C J | KV -40°C J | |
| 590 | 800 | 28 | 90 | 70 | |

Mechanical tests of the joints: bend test of the root and face (min specified angle 120°; mandrel diameter 5 x thickness of the plate), Rm, KV and HRC tests have been made according to Det Norske Veritas Rules Corrosion tests have been made according to DNV Rules Pt.2 Ch.3 Sec.2 – D-200 – Method of Examination and ASTM G48-76 Method A). Ferrite share has been made according to DNV Rules Pt.2 Ch.3 Sec.2 D203 – acc. to ASTM E562 Specification. An influence of the heat input of duplex steel submerged arc welding on a type and quantity of welding imperfections of butt joints have been determined by means of X-Ray tests. In this order ratio of quantity of radiographs with the negative results – RN to the complete quantity of radiographs RC was established as index of the welds defectiveness RC. Radiographs were classified basing on PN-12517 and PN-EN 25817 – Arc-Welded Joints in Steel – Guidance on Quality Levels for Imperfections. In the second stage of the experiment joints of the plates 10 meters long were done according to established edge preparation and thickness: 10 - 15; 16 - 21; 22 - 27; 28 - 32 mm. Fraction index of the welding imperfections types occurring in joints WR in relation to the complete quantity of X-ray testing was determined. Submerged welds of duplex steel were subject to the visual and X-Ray examinations on the basis of criteria and requirements of Polish – European Standards. Welds should meet criteria of quality level B according to PN-EN 25817. X-rays apparatus Baltospot Ceram 235 carried out tests.

$$W = \frac{RN \times 100}{RC}[\%] \quad (2)$$

$$WN = \frac{RW \times 100}{RN}[\%] \quad (3)$$

$$WR = \frac{RW \times 100}{RC} \quad (4)$$

where: W [%] – percentage index of welds defectiveness, RN [pcs.] – quantity of tests with negative result, RC [pcs.] – complete quantity of radiographs, RW – quantity of radiographs with a specific type of weld imperfection [1].

The mechanical properties test results are presented in Tables 12-14. The weld shape and imperfection (Table 15) test results are presented in Figures 11-15.

Results of the X-Ray tests of welds made with a usage of maximum hit input HI ≤ 2.5; HI ≤ 3.0; HI ≤ 3.5; HI ≤ 4.0kJ/mm proved lack of the negative influence of this l hit input value on duplex steel joints quality. Results of the mechanical properties tests of joints fulfil the requirements regarding duplex steel joints. Next the tests with usage of two heat input values: HI ≤ 2.5 and HI ≤ 3.0kJ/mm have been carried out in production conditions. It was affirm the lack of inadmissible welding imperfection in the joints.

Types of weld imperfections found as the tests result are presented in Table 15. The experiment proved, that assumed welding heat input up to 2.5 kJ/mm while submerged arc welding with above mentioned edge preparation led to occurrence of many inadmissible welding imperfections. Application of welding heat input of about HI = 3 kJ/mm caused radical decrease in welds defectiveness. Figs. 12-14 represents percentage occurrence index of kinds of welding imperfections in a joint calculated according to e.g. 2 - 4.

Table 12.
Rm of tested plate of 26 mm thickness [2]

| Heat input HI [kJ/mm] | Rm Average value MPa | Fracture place |
|---|---|---|
| HI ≤ 2.5 | 690 | Fracture in the parent material |
| HI ≤ 3.0 | 750 | Fracture in the parent material |
| HI ≤ 3.5 | 747 | Fracture in the parent material |
| HI ≤ 4.0 | 744 | Fracture in the parent material |

Table 13.
KV of tested plate of 26 mm thickness [2]

| Heat input HI [kJ/mm] | Average value of KV, J for notch localization | | | |
|---|---|---|---|---|
| | Weld metal | Fusion line FL | HAZ FL + 2 mm | HAZ FL + 5 mm |
| HI ≤ 2.5 | 120 | 90 | 105 | 119 |
| HI ≤ 3.0 | 115 | 135 | 220 | 200 |
| HI ≤ 3.5 | 80 | 148 | 160 | 148 |
| HI ≤ 4.0 | 78 | 155 | 218 | 184 |

Table 14.
HV5 of tested plate of 26 mm thickness [2]

| Heat input HI [kJ/mm] | HV5 | | | | | |
|---|---|---|---|---|---|---|
| | Parent material | | Weld metal | | HAZ | |
| | min | max | min | max | min | max |
| HI ≤ 2.5 | 235 | 261 | 248 | 269 | 244 | 273 |
| HI ≤ 3.0 | 233 | 272 | 255 | 284 | 238 | 277 |
| HI ≤ 3.5 | 237 | 248 | 263 | 290 | 241 | 269 |
| HI ≤ 4.0 | 240 | 262 | 259 | 288 | 254 | 281 |

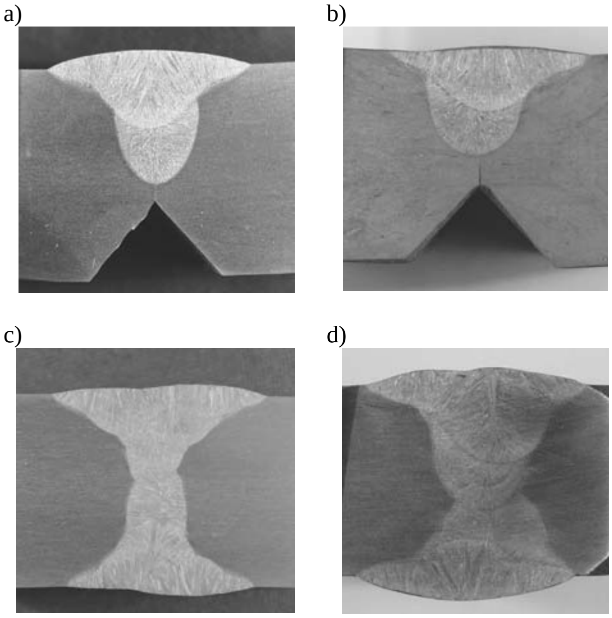


Fig. 11. Shape of the weld bead of plate of 26 mm thickness: a) HI ≤ 2.5kJ/mm, b) HI ≤ 3.0kJ/mm; plate of 30 mm thickness; c) HI ≤ 2.5 kJ/mm, d) HI ≤ 3.0kJ/mm [2]

Table 15.
Welding imperfection found in the test [2]

| Type | Marking |
|---|---|
| gas cavity | 2011 |
| slag inclusion | 3012 |
| linear slag | 3011 |
| lack of side fusion | 4011 |
| lack of joint penetration in two-sided weld | 402 |
| longitudinal crack in weld | 1011 |
| root and face undercut | 5011/5012 |

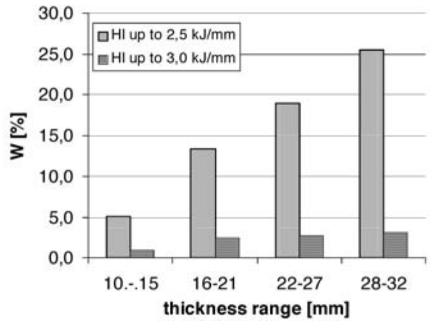


Fig. 12. Fraction of welding imperfections W – acc. to Equation 2 in X-rays testing for HI ≤ 2.5 kJ/mm and HI ≤ 3.0 kJ/mm [2]

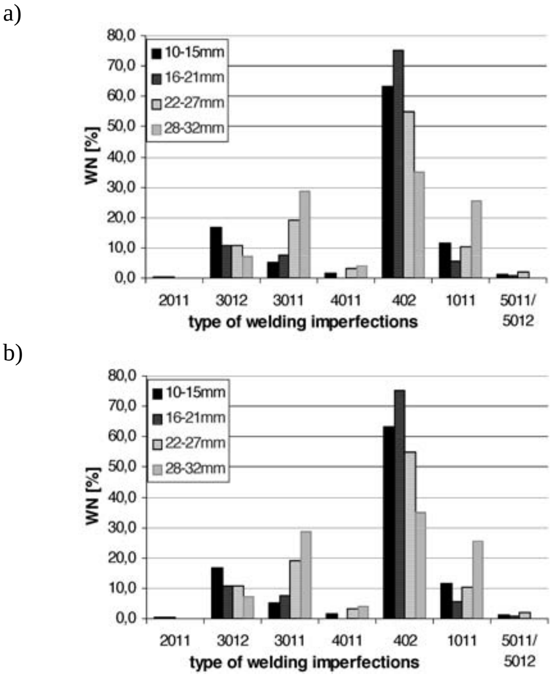


Fig. 13. Fraction of welding imperfections in X-rays testing with negative result WN – acc. to Equation 3 for a) HI ≤ 2.5kJ/mm, b) HI ≤ 3.0 kJ/mm [2]

The tests proved that welding with heat input up to 3.0 kJ/mm reduced welding imperfections occurring in joints, e.g. slag, lack of joint penetration, and for plates of 10-23 mm thickness - incomplete fusion and cracks, as well as decreased radically occurrence of other welding imperfections. On the base of the tests results it can be stated, that in terms of the duplex steel welding quality higher heat input improves quality of welds. It has an important influence on costs of repair. The problem is limitation of quantity of heat introduced into the weld causing a necessity to use many operations to ensure high quality of the joints and the following of basic principles of duplex steel welding process, as: stable welding parameters, proper wire feeding, correct weld shape, correct assembly of elements to be joint, lack of contamination like dust, point, oil and humidity, minimizing of welding stresses.

a)

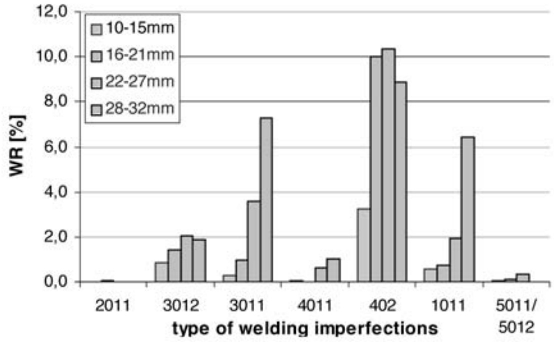


b)

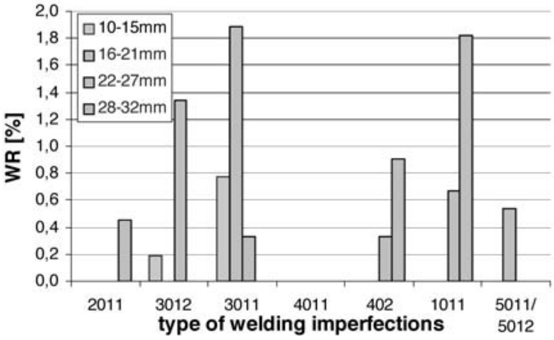


Fig. 14. Fraction of welding imperfections in X-rays testing with negative result WR – acc. to Equation 4, for a) HI ≤ 2.5kJ/mm, b) HI ≤ 3.0 kJ/mm [2]

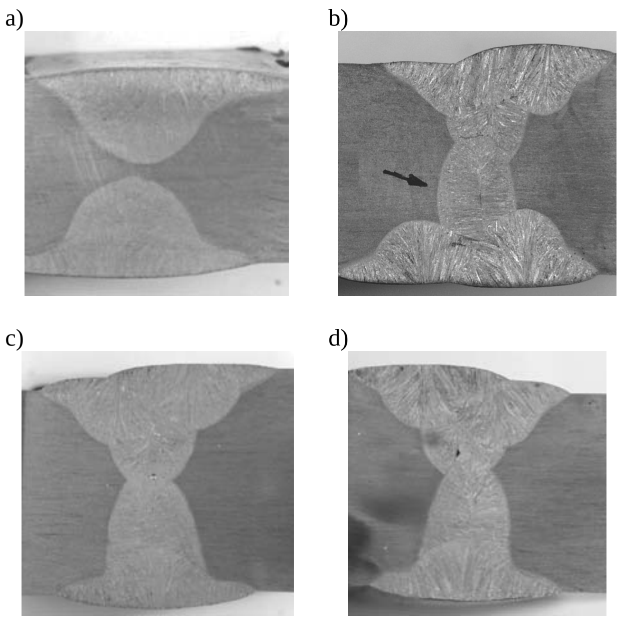


Fig. 15. Macroscopic image of a weld with a) lack of joint penetration, b) crack, c) pinhole, d) slag [2]

## 9. Corrosion resistance of SAW duplex joints welded with high heat input

In order to compare requirements applicable to welded joint specified in the Det Norske Veritas Rules and the impact of the welding heat input occurring at SAW welding of duplex steel UNS S31803 on the corrosion resistance of welded joints, a number of tests were performed for specifying maximum value of the welding heat input at which the welded joint loses its corrosion resistance or strength (mechanical) properties.

In joints with the above mentioned a series of butt joints on plates of 30 mm thickness were executed where the applied heat input of welding exceeded the 2.5 kJ/mm value. Beads of butt joints with butt weld were made using maximum value of welding heat input, starting from 3.0 kJ/mm and increasing every 0.5 kJ/mm up to value 5 kJ/mm, in flat welding position. All welds were tested for corrosion resistance and the weld metal microstructure analysis was performed, as well as ferrite fraction was determined.

In addition, destructive and non-destructive testing of butt joints with butt-welded was performed, with heat input of welding exceeding the recommended value HI 2.5 kJ/mm. In order to determine the influence of the multiple-pass welding/bead welding on the ferrite fraction, and on the corrosion resistance, welded joints of various thickness bevel pate thickness 9, 14, 28 mm and with constant value of welding heat input on level 1.35 kJ/mm were executed, in which filler pass and final layers were made by submerged arc welding in horizontal-vertical position. All butt weld joints were tested for corrosion resistance and the weld metal microstructure analysis was performed, as well as ferrite fraction t was determined.

The duplex steel UNS S31803 used for testing was characterized by similar chemical composition and strength parameters as given in Table 10 and the structure as on Fig. 16. Filler metal used for welding of test joints: flux cored wire of 3.2 mm diameter, grade 2205, made by Avesta Company, with the flux 805, whose strength parameters and chemical composition are given in Table 11.

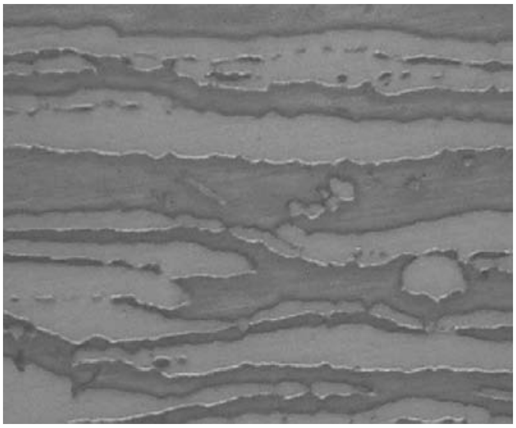

Fig. 16. Microstructure of the parent material, steel UNS S31803 used in the experiment; ferrite - dark phase, austenite - bright phase; ferrite (α) volume fraction 48% [3]

All butt joints with butt weld were subjected to the following non-destructive testing [3]:

- visual examinations according to the required quality level B acc. to the Polish – European Standards PN-EN 25817,
- X-Ray examinations acc. to the Polish – European Standard PN-EN 12062 with the required quality level B as per the Polish – European Standard PN-EN 25817.

The following destructive testing of joints were done too:

- macroscopic examination [3],
- bend test of face from the first and second side of welding at a criterion in specified bend angle 120º; mandrel diameter 5 x thickness of the test plate,
- impact test- min KV = 27J w -20 °C,
- tensile test – min Rm = 620 MPa,
- corrosion resistance tests were carried out according to ASTM G48 Method A test and guidelines of Det Norske Veritas and American Bureau of Shipping. The specimens (76×24×16.5) were dipped in ferric chloride reagent (100g $FeCl_3 \cdot 6H_2O$ in 900 ml $H_2O$). Etching was performed at temperature 295 ± 2 K. The test duration was 24 hours. According to guidelines of Det Norske Veritas and American Bureau of Shipping the specimen mass loss smaller than 20 mg is acceptable,
- microstructure examination and ferrite share determination were performed using optical microscopy. Colour etching by Murakami's reagent (KOH – 10g; $K_3Fe(CN)_6$ – 10g; $H_2O$ – 100ml) was used to produce contrast between the primary phases (ferrite and austenite) and to reveal the presence of secondary phases precipitates. A programme for analysing digital images VISILOG 4 determined the ferrite and secondary phases content. Hardness tests HV5 were performed according to EN 288 in the cross section of the welded joints in the heat-affected zone area. Six measurement points have been chosen in the face of the weld line, and the root of weld line. More detailed studies of the hardness alternation were performed using Vickers HV0.02 method. Thirty measurements of each phase in different the heat-affected zone areas (face, root) of the samples, and in different aging conditions were performed.

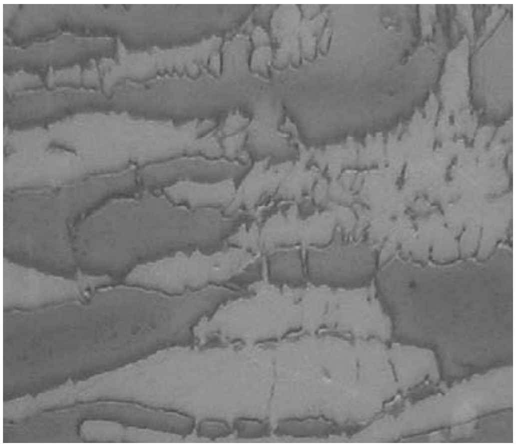

Fig. 17. Microstructure of the HAZ; heat input HI = 4.5; ferrite - dark phase, austenite - bright phase; ferrite (α) volume fraction 59% [3]

Butt joints with butt weld of test plates were welded using maximum heat input at a level of HI ≤ 3.0; HI ≤ 3.5; HI ≤ 4.0; HI ≤ 4.5; HI ≤ 5.0. The X-Ray examinations of butt-welded joints were performed acc. to the European standard EN12062 with the required quality level B as per EN 25817 standard (positive test results).

The destructive testing were performed as per DNV Rules. The performed bend test of face from the first and second side of welding: (min specified bend angle 120º; mandrel diameter 5 x thickness of the test plate, were positive. The metallographic examination shown ferritic – austenitic structure of the welds and HAZ and an appearance of secondary austenite in some tested joints (Figs. 17-22).

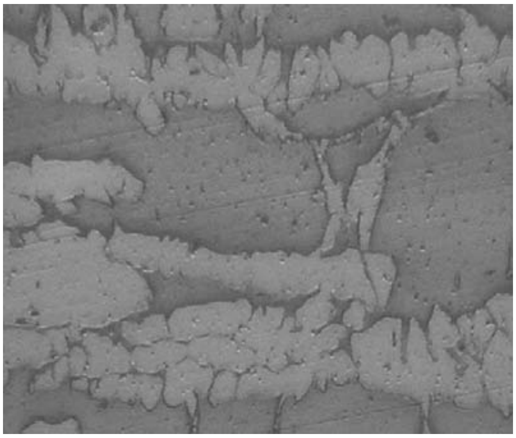

Fig. 18. Microstructure of the HAZ; heat input HI = 4.5; ferrite - dark phase, austenite - bright phase; ferrite (α) volume fraction 57% [3]

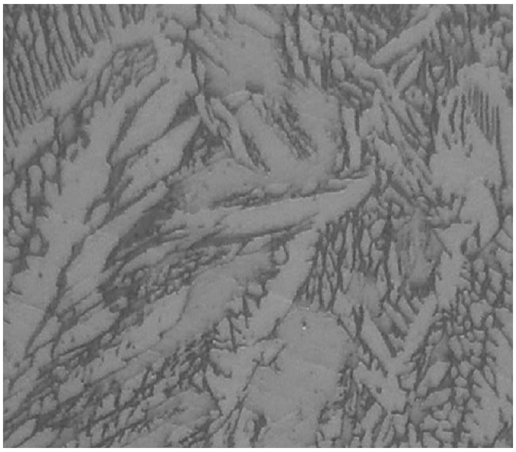

Fig. 19. Microstructure of the weld; heat input HI = 4.5; ferrite - dark phase, austenite - bright phase; ferrite (α) volume fraction 47% [3]

The result of ferrite fraction tests, shown on Figs. 23 and 24 corresponded the acceptance level acc. to DNV rules. A tensile test of the joints was in all cases higher, than 620 MPa - required minimum value. Charpy V-notch specimens and hardness tests Vickers method – results were presented on the Figs. 25 and 26 (all tests results were positive) and the fracture images of welds and HAZ were ductile Figs. 27 and 28. Results of the corrosion resistance tests are presented in Tables 16 and 17. Samples subjected to corrosion resistance testing were free of any corrosion traces (Figs. 29 and 30).

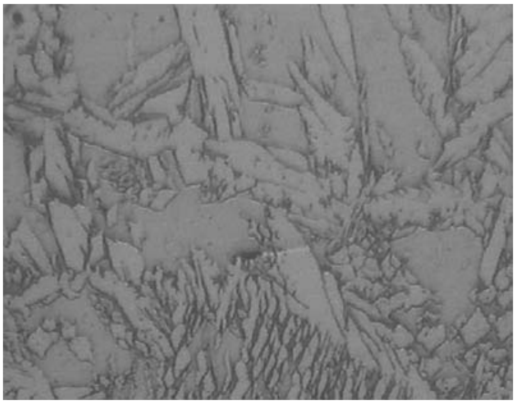

Fig. 20. Microstructure of the weld; heat input HI = 4.5; ferrite - dark phase, austenite - bright phase, needles of secondary austenite; ferrite ($\alpha$) volume fraction 54% [3]

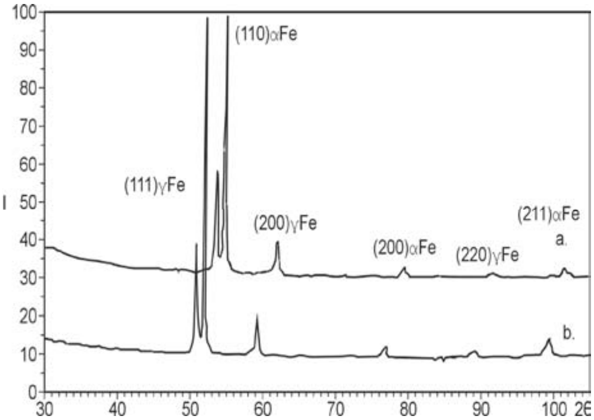


Fig. 21. Diffraction image of the weld, heat input: a - HI = 3.0; kJ/mm, b - HI = 4.5; kJ/mm; $\alpha$Fe – ferrite, $\gamma$Fe - austenite [3]

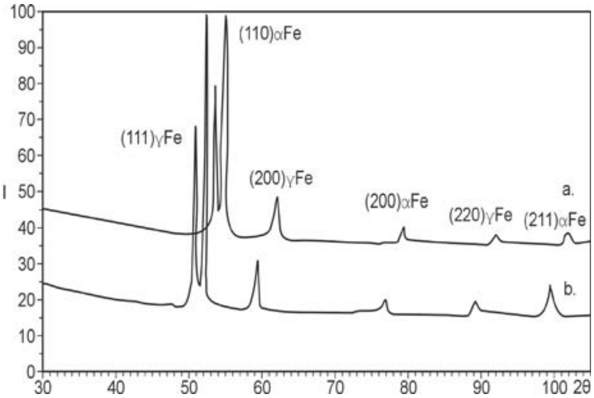


Fig. 22. Diffraction image of the HAZ, heat input: a - HI = 3.0 kJ/mm, b - HI = 4.5; kJ/mm; $\alpha$Fe – ferrite, $\gamma$Fe – austenite [3]

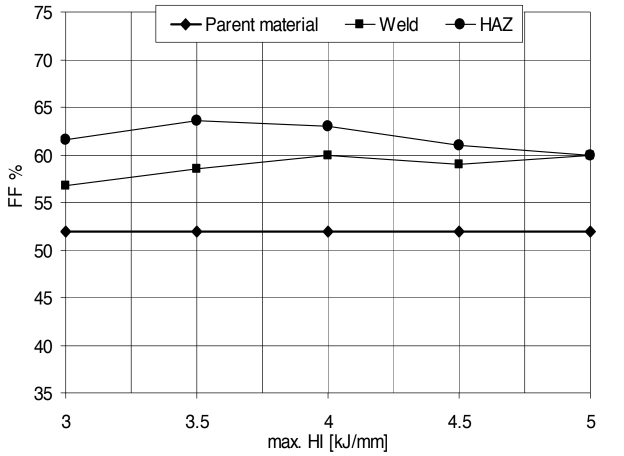


Fig. 23. Average values of ferrite volume fraction FF% in butt joints with butt welds [3]

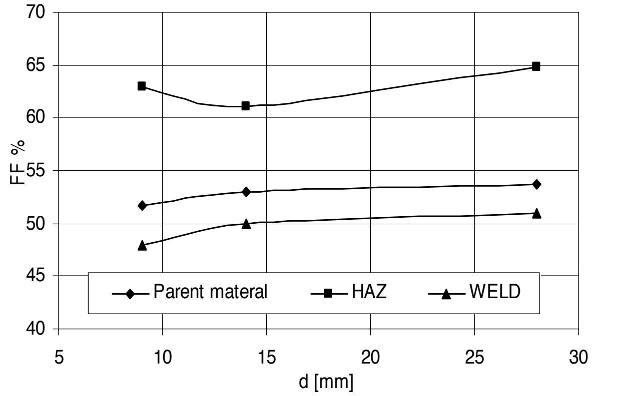


Fig. 24. Average value of ferrite volume fraction FF% in butt joints with butt weld in the plate thickness - d function, heat input HI = 4.5 kJ/mm [3]

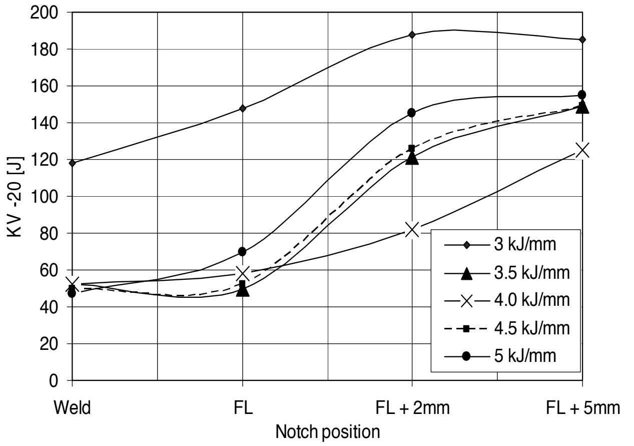


Fig. 25. Average value of KV J of butt joints with butt welds (min KV = 27J at -20 $^{o}$C) [3]

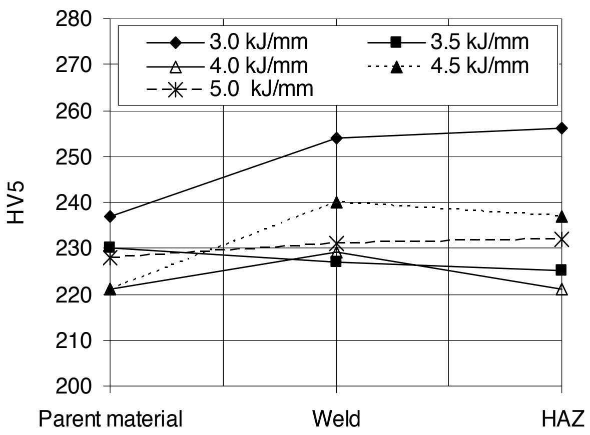


Fig. 26. Average values of HV5 hardness of butt joints with butt welds [3]

Table 16.
Average value of mass loss of butt-welded joints after corrosion resistance testing; plate thickness 14 mm [3]

| Max. hit input, kJ/mm | Average value of mass loss of butt-welded joints after corrosion resistance testing, mg |
|---|---|
| 3.0 | 1.15 |
| 3.5 | 1.12 |
| 4.0 | 1.10 |
| 4.5 | 1.07 |
| 5.0 | 1.05 |

Table 17.
Average value of mass loss of butt-welded joints after corrosion resistance testing, Max. hit input 3.5 kJ/mm [3]

| Plate thickness, mm | Average value of mass loss of butt-welded joints after corrosion resistance testing, mg |
|---|---|
| 9 | 1.02 |
| 14 | 1.12 |
| 28 | 1.25 |

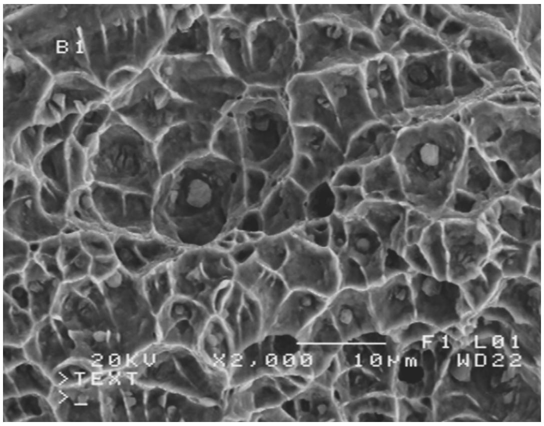


Fig. 27. Ductile fracture image of the HAZ, heat input HI = 4.5 kJ/mm [3]

Fig. 29. Macrostructure of the weld after corrosion test; heat input 3.0 kJ/mm; no pitting corrosion [3]

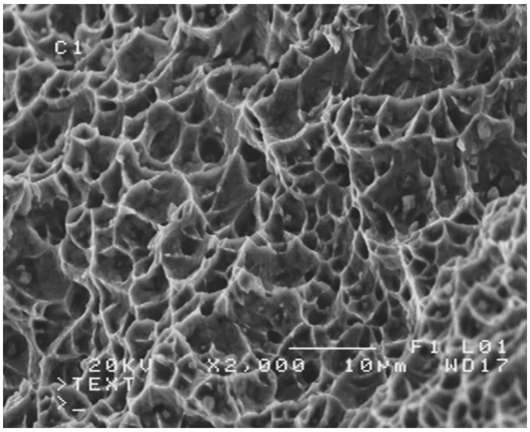


Fig. 28. Ductile fracture image of the weld, heat input heat input HI = 3.0 kJ/mm [3]

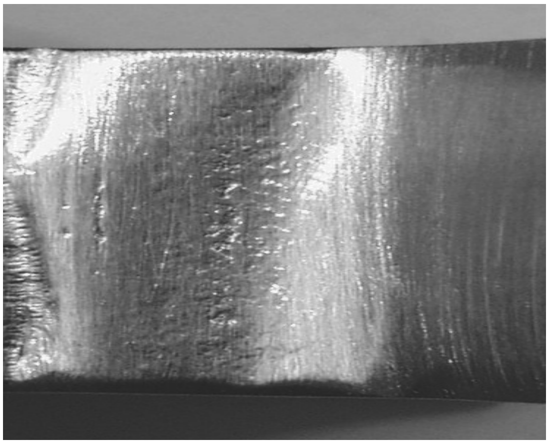

Fig. 30. Macrostructure of the HAZ after corrosion test; heat input 4.5 kJ/mm; no pitting corrosion [3]

## 10. Microstructure and corrosion resistance of the duplex steel wide-gap welded joints

When analysing in recent years the world industry dealing in building of large - size constructions, including chemical cargo carriers, the growing tendency to use duplex stainless steel grades. Building of large - size constructions (of duplex steel) is of multi-stage character. At different building stages there occurs necessity to execute welded joints in fixed positions. These positions as a rule enforce using maximum welding heat input, which results first of all from limited possibility to increase the speed of welding in these positions. Publications relating to duplex steel welding indicate that the recommended welding heat input should range from 0.5 to 2.5 KJ/mm [4].

The need to extend this range is associated with welding of 3D sections at assembly in fixed positions (mainly in vertical position). When building constructions of this type for butt joints usually mechanized welding is applied using automatic welding equipment (e.g. of Bug-o matic type), fluxcored wires, with active gas shield (Fig. 31).

a)

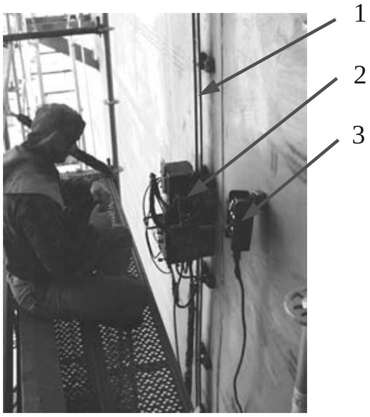


b)

Fig. 31. Welding of butt type joints of large-size constructions, a – before welding, during welding 1 – guide rail, 2 - automatic welding machine, 3 – control desk [4]

The automatic welding equipment moves along a guide rail, which is fixed, to plate by means of magnets. When joining sections, one-side welding on ceramic backings is used. The root run of the weld penetration layer is formed then by means of flat ceramic backing which is then placed inside the section.

After the weld execution the backing is removable. The obtained root run of the weld does not require execution of any auxiliary operations, e.g. grinding off (Fig. 32).

Plate edges in such a welding method are bevelled at „1/2V", which results in weld groove of „V" geometry (shape). One-side welding with preparation of weld groove at „V" is usually applied for plates of thickness ranging from 8 to 18 mm.

a)

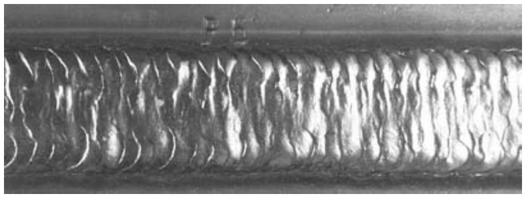

b)

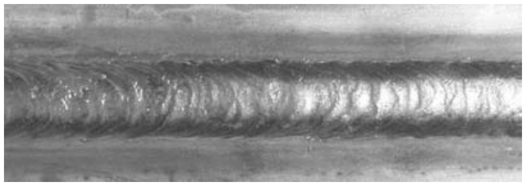

Fig. 32. View of weld executed by one side welding in PF (vertical - up) position (the weld penetration layer is formed on ceramic backing): a) the weld face, b) the root run of the weld [4]

One-side welding of plates up to 20 mm thickness in large-size constructions has and advantage over both-sides welding due to:

- easy access only from one side (from the other side there is fitted the whole supporting structure consisting usually of stiffening of I and II type
- possibility of automated execution of all weld layers,
- advantageous shape of the obtained weld penetration layer, preventing occurrence of hot cracks,
- reducing of labour demand for welded joint execution,
- reducing of labour demand necessary for edge treatment,
- improvement of conditions in welder – operator's working environment.

The drawback is a possibility of occurrence of angle distortions of the welded joint. However, using appropriate can solve this problem welding technology, consisting mainly in proper welding sequence and special stiffening of the welded joint.

It is the root face gap that is the basic parameter characterizing the weld groove geometry, influencing the quantity of heat input, and as a result – the properties of the welded joints. For a butt type welded joint at one-side welding the root face gap (distance) ranging from 4 do 6 mm is assumed [4]. The limits values given result directly from experience in execution of similar welded joints. They make a compromise between obtaining correct strength and microstructural properties and the optimum performance of the welding process (optimisation in terms of economic profitability – cost - effectiveness).

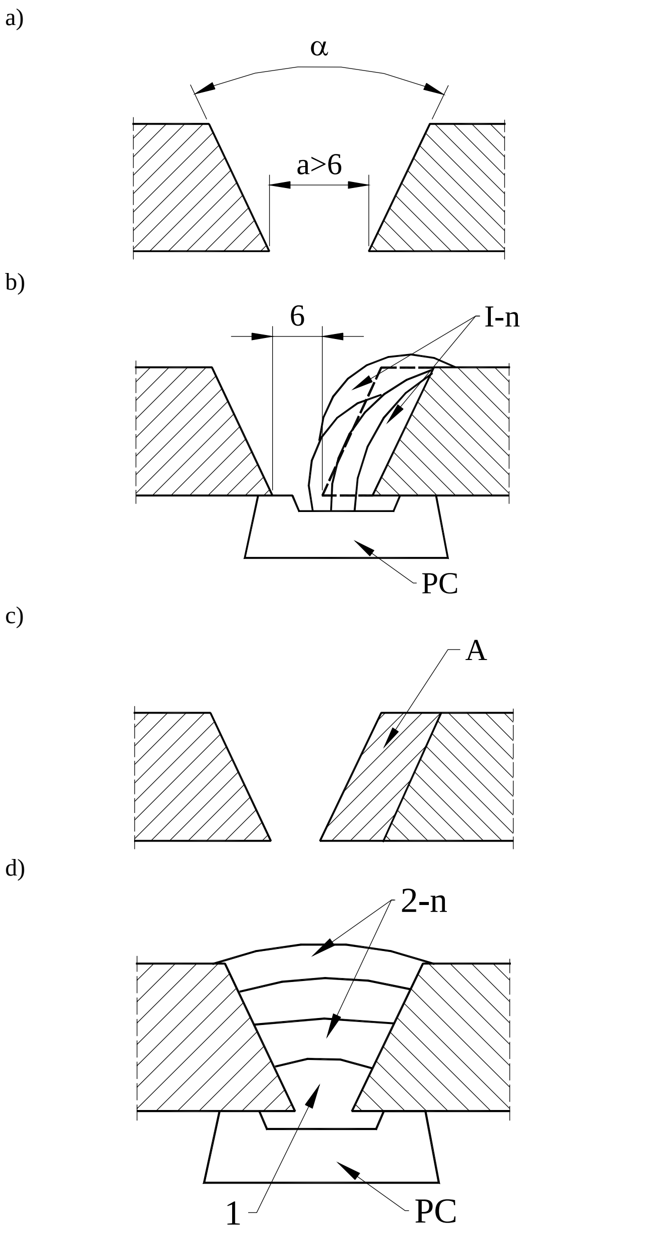


Fig. 33. Scheme of one-side welding combined with repair (reconstruction) of the plate edge by surfacing, where: a - root face gap, α-groove angle, PC-ceramic backing, b - repairing the weld groove prior to welding, c -padding welds, A - surfaced area after performed grinding off, d – weld, 1 - the weld root layer, 2-n- filler passes and face layer [4]

In case of reducing the root face gap to a less than 4 mm size for one-side welding on ceramic backings there appear some difficulties (problems) with execution of the weld penetration layer. The root run of this layer does not comply with requirements of the B quality level as per PN-EN 25817 standard and DNV rules relating to the shape and surface welding defects and imperfections. Execution (welding) of this layer in PF (vertical - up) position is made difficult (hindered) due to accumulation of heat in a small area. It may result in occurrence of local imperfections in form of sagging puddles, lack of fusion caused by a great number of connections (areas of welding operation starting and ending) of the weld penetration layer. Then the tendency of increased welds defectiveness occurs. Usually it results in increase of the total cost of the construction execution by extending the inspection scope (both interoperation and final ones). The aim is that the obtained minimum value of the root face gap before and during welding is not less than 4 mm.

The maximum value (6 mm) results mainly from experience gained by welding materials producers as regards obtaining of strength and microstructural parameters of welded joints. Due to scarcity of available literature relating to welding of large-size constructions, where the main problem is maintaining of appropriate execution tolerances, in case of exceeding the maximum value of the root face gap being equal to 6 mm it is recommended to repair the weld groove prior to welding.

This repair may be performed in two ways. The first one consists in replacement of part of the plate. However, in this case we are dealing with an additional weld joining the new fragment with the old one. Therefore this way is applied only as the last resort. The second step consists in reconstruction of the plate edge by surfacing (Fig. 33).

The process of preparation of weld groove with the plate edges surfacing is a complicated and multistage process. It comprises not only reconstruction of the plate edge but also its proper preparation for welding. Due to necessity to use minimum parameters, surfacing is characterized by high defectiveness rate.

The following defects occur very frequently: lack of fusion and non - metalic solid inclusions. Execution of correct padding weld of the plate edge requires very high skills. It is a long-lasting and cost-intensive process. After the stage of the plate edges surfacing (Fig. 34) the executed padding weld cannot be inspected.

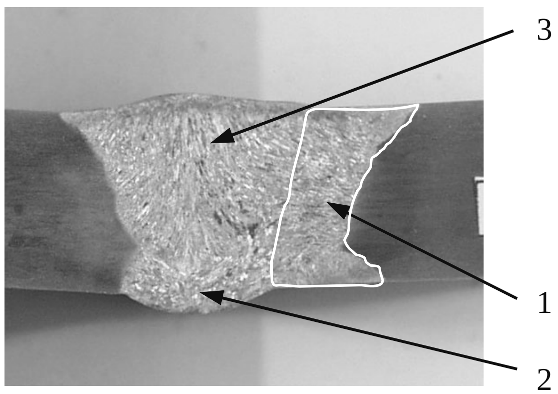


Fig. 34. Macro - image of the welded joint macrostructure with visible repair of the plate edge by surfacing, where: 1 - surfaced layer, 2 - weld root layer, 3 - filler passes and face layer [4]

The only available methods are visual examinations and dye penetrates examinations, but they are applicable only to examination of surface welding defects and imperfections. There is no possibility to check the padding weld inside. The stage of the padding weld inside examination can be performed only on completion of the process of grinding off and welding of the whole joint (Fig. 35), which in case of large-size constructions is unacceptable.

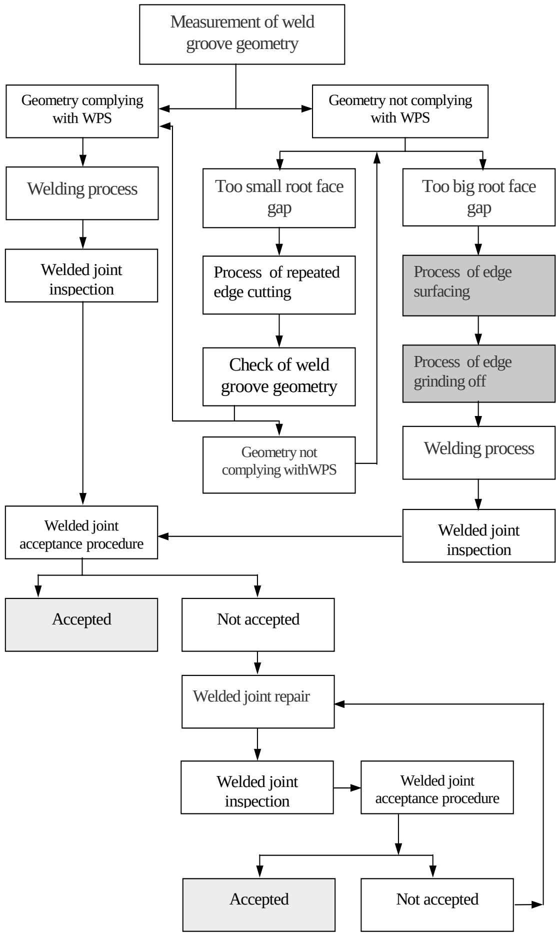


Fig. 35. Schematic presentation of stages of the welded joint execution – from the moment of the weld root geometry measurement to acceptance inspection of the welded joint [4]

The 2 mm range of root face gap tolerances, giving the dimension ranging from 4 to 6 mm, is too narrow in case of welding joints of total length exceeding 5 m. For execution of such a large-size construction, maintaining such a narrow tolerance range of the basic parameter of the weld groove is practically impossible and in many cases these dimensions are exceeded. It results most often from tolerances assumed (accepted) for particular operations. So e.g. the line marking-off tolerance range is ±1 mm.

The plasma arc cutting tolerance range is ±2 mm. Measuring errors resulting from measuring instruments are contained in ±1 mm tolerance (allowance). In some cases values of tolerances for particular operations are summed up (tolerance stack-up) and the obtained dimension of the root face gap is exceeded. Most often the plus tolerances are extended, i.e. the dimension of the root face gap is higher than 6 mm (within 6 - 10 mm limits).

Thus the surfacing process is consciously introduced into the process of basic execution of the welded joint. Generally in welding procedures in case of gaps >6 mm the surfacing of plate edges prior to welding is applied [4].

In order to execute one-side welded joints without using the edge surfacing process it is necessary to extend the range of root face gap tolerances.

The research and tests conducted of the Szczecin University of Technology in cooperation with the Szczecin New Shipyard permitted to determine the impact of the wide-gap welding, with increased root face gap, on structure and corrosion properties of the welded joints executed on duplex steel by one-side welding on ceramic backings.

Welding tests were performed based on the elaborated experiment plan. 9 welded joints of 1.000 mm length each were executed.

Three-plate thickness was assumed. For each of them welding with root face gap of the weld groove, equal to 6, 8 and 10 mm, was performed. Table 18 presents characteristics of welded joints [4].

Table 18.
Characteristics of executed welded joints [4]

| No. of the weld | Plate thickness mm | Root face gap mm | Groove angle deg | Welding position | Welding heat input range |
|---|---|---|---|---|---|
| 1 | 9 | 6 | 45 | PF | 2.02-2.35 |
| 2 | 9 | 8 | 45 | PF | 2.34-2.80 |
| 3 | 9 | 10 | 45 | PF | 1.58-2.58 |
| 4 | 14.5 | 6 | 45 | PF | 1.80-2.94 |
| 5 | 14.5 | 8 | 45 | PF | 1.94-3.51 |
| 6 | 14.5 | 10 | 45 | PF | 1.94-3.94 |
| 7 | 18.5 | 6 | 45 | PF | 1.63-3.55 |
| 8 | 18.5 | 8 | 45 | PF | 2.13-3.82 |
| 9 | 18.5 | 10 | 45 | PF | 2.37-3.93 |

Particular joints were executed using FCAW – Flux Cored Arc Welding – 136 - one-side welding with the weld penetration layer on ceramic backing on plates (thickness g = 16.5 mm) made of duplex steel UNS S31803 using filler metal DW329AP/ C1 (100%$CO_2$).

Non-destructive testing of welded joints was intended for the evaluation of quality of welded joints. The requirements specified for the B quality level as per PN-EN 25817 standard were assumed as a criterion.

Visual examinations were performed based on the PN-EN 970 standard. All the welded joints covered by the analysis complied with the requirements for the B quality level. Table 19 presents appearance of the weld faces and the root runs of particular welded joints with characteristic dimensions given.

On the basis of the performed visual examinations the following was found out:

- increase of the root run reinforcement width (maximum by 2.5 mm) with increase of the root face gap,
- increase of the root run reinforcement width (maximum by 4.5 mm) with increase of the root face gap,
- occurrence of undercutting of the root run of the weld on welded test plates on both sides, with root face gap exceeding

8 mm. Permanent character of these undercuts shows that it is necessary to modify the construction of ceramic backing (due to insufficient working area). These undercuts are easily removable because of small depth (less than 0.3 mm). All the test plates complied with the requirements for the B quality level as per PN-EN 25817 standard.

Table 19.
Dimensions of weld faces and the root runs of executed welded joints [4]

| No and dimension of the weld mm | Macro - image of the weld face |
|---|---|
| No 1<br>weld face width 18<br>weld face height 1<br>root run width 12.5<br>root height 2 | 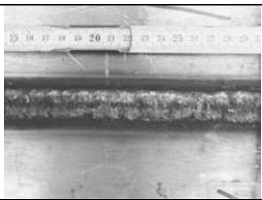 |
| No 2<br>the weld face width 19.5<br>weld face height 1.5<br>root run width 13<br>root height 1.5 | 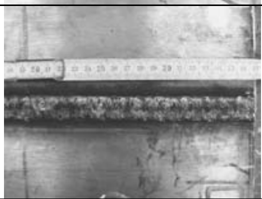 |
| No 3<br>the weld face width 21<br>weld face height 1.5<br>root run width 15<br>root height 2 |  |
| No 5<br>the weld face width 23<br>weld face height 0.7<br>root run width 12.5<br>root height 2 |  |
| No 6<br>the weld face width 24.1<br>weld face height 1<br>root run width 14.5<br>root height 1.5 | 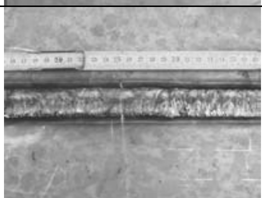 |
| No 8<br>the weld face width 25.5<br>weld face height 2<br>root run width 13<br>root height 2 | 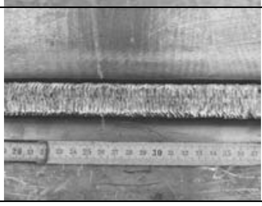 |

Tests of the ferrite content were performed with ferritescope (Fig. 36). This instrument, for measuring the ferrite content, makes use of phenomenon of magnetic induction. The examinations covered measurement of the ferrite content at the side of weld face, heat affected zone (HAZ) and base material. The width of heat-affected zone (HAZ) was assumed experimentally, i.e. it was specified as the area from the fusion penetration line to 2 mm deep into base material. 20 measurements were performed in each of the zones. Examination results are listed in Table 20 and in Fig. 37.


Fig. 36. Complete equipment for measuring the ferrite content, 1 - calibration standards, 2 – connecting cable, 3 - ferritescope [4]

Table 20.
Examples of the tests of ferrite content results of investigated welding joints [4]

| No. of the sample | Area of the test | Approximate ferrite content, % |
|---|---|---|
| | Parent material | 39 |
| 1 | HAZ | 62 |
| | Weld | 49 |
| | Parent material | 44 |
| 2 | HAZ | 59 |
| | Weld | 45 |
| | Parent material | 40 |
| 3 | HAZ | 56 |
| | Weld | 38 |
| | Parent material | 46 |
| 4 | HAZ | 64 |
| | Weld | 47 |
| | Parent material | 41 |
| 5 | HAZ | 55 |
| | Weld | 41 |
| | Parent material | 59 |
| 6 | HAZ | 40 |
| | Weld | 55 |
| | Parent material | 57 |
| 7 | HAZ | 39 |
| | Weld | 46 |
| | Parent material | 40 |
| 8 | HAZ | 52 |
| | Weld | 39 |
| | Parent material | 45 |
| 9 | HAZ | 61 |
| | Weld | 39 |

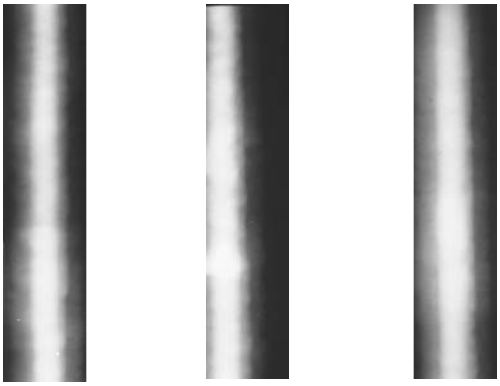

Fig. 37. Correct X – ray images of the sample No. 9 in different areas, done by Technic - Control Sp. z o.o. Szczecin [4]

All test pieces underwent X-ray examinations, which were performed, based on the PN-EN 1435:2001 standard. The B quality level as per PN-EN 25817 standard was assumed as a criterion.

On the basis of the performed tests of the ferrite content the following was found out:

- correct ferrite content in all examined test plates (acc. to relevant requirements of DNV rules).
- the lowest ferrite content (share) for test plates welded with 10 mm root face gap for three examined test plates,
- decrease in ferrite content together with increase of the root face gap (welding heat input increase),
- considerable stability of individual measurements results, especially for measurements performed in the weld face area.
- all the tested welded joints comply with the required quality level – stringent requirements, B quality level.
- increasing of the root face gap to 10 mm in butt welded joints does not have an adverse effect on quality level.
- in each of the cases covered by the analysis the basic detected imperfections were single gas pores of size much smaller than the limit values for B quality level.
- no defects in form of cracks or lack of fusion were found.

On the basis of the performed analysis of the examination results there is no relation between the root face gap (range of its value changes) and the obtained quality of the joint.

As a result of the metallographic analysis, the microstructure of areas of welded joints, executed depending on welding parameters, was determined. In order to reveal the microstructure of areas (zones) of duplex steel welded joints, chemical and electrolytic etching of microsections was applied.

The microsections were subjected to macroetching in Murakami reagent of the following composition:

- potassium hydroxide KOH -10g
- potassium ferricyanide $K_3Fe(CN)_6$ -10g
- distilled water $H_2O$ -100ml

This reagent dyes ferrite dark brown, whereas austenite remains bright. Metallographic examination was performed using light microscope at x 400 enlargement, according to recommendations of DNV rules Pt.2 Ch.3 Sec.2 D203. Ferrite volumetric share was determined with net counting method, according to ASTM E562 standard and as per guidelines in DNV Rules Pt.2 Ch.3 Sec.2 D203.

In all the examined test pieces presence of only ferrite and austenite was identified (Figs. 38-41 and 43-47). In the diagrams only selected examination results are presented which are typical of all the test pieces.

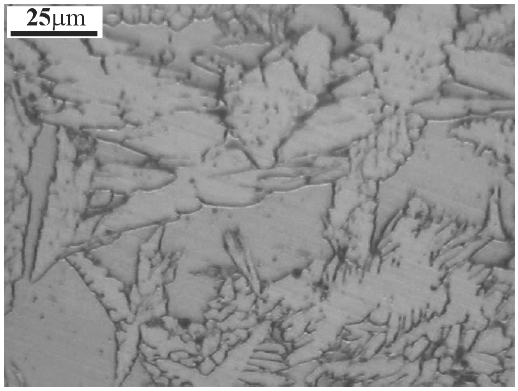


Fig. 38. Typical microstructure of examined weld exemplified by specimen No. 3, face side, x 400 magnification, ferritic – austenitic structure, average value of ferrite share 54% [4]

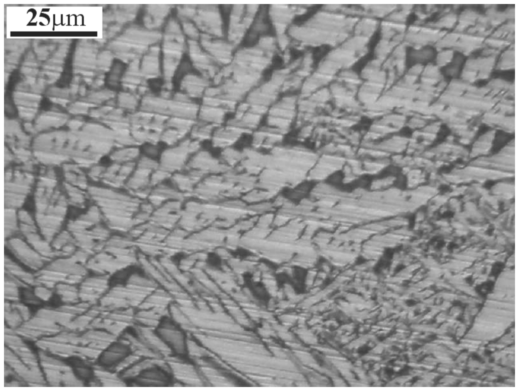


Fig. 39. Typical microstructure of examined of the weld exemplified by specimen No. 9, face side, x 400 magnification, ferritic – austenitic structure, average value of ferrite share 44% [4]

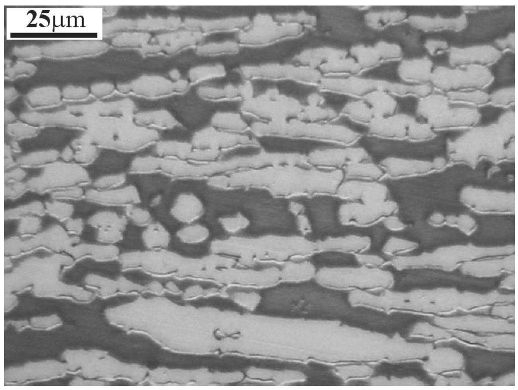


Fig. 40. Typical microstructure of examined of the HAZ exemplified by specimen No. 3, root side, x 400 magnification, ferritic – austenitic structure, average value of ferrite share 43% [4]

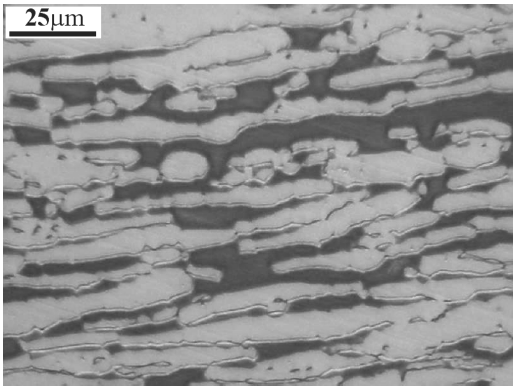


Fig. 41.Typical microstructure of examined of the HAZ exemplified by specimen No. 9, root side, x 400 magnification, ferritic – austenitic structure, average value of ferrite share 35% [4]

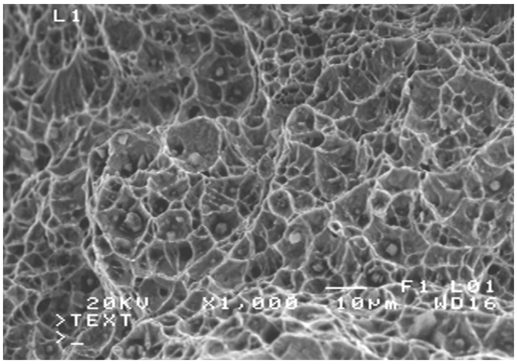


Fig. 42. Ductile fracture of the sample No. 9 weld [4]

The HV10 hardness tests were performed according to the guidelines in the PN-EN 288 – 3, p. 7.4.5. standard. The microhardness measurements were performed using Vikcers method at 25 g loading.

The value of hardness of all test pieces did not exceed 350 HV, hardness of austenite and ferrite in the tested areas of welded joints was similar, and hardness of austenite was slightly higher than that of ferrite (Tables 21 and 22).

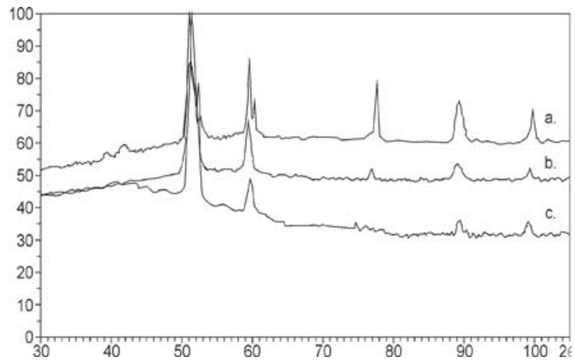


Fig. 43. Specification of diffraction patterns of welds of the samples: a - No. 1, b – No. 5, c – No.9, ferrite and austenite [4]

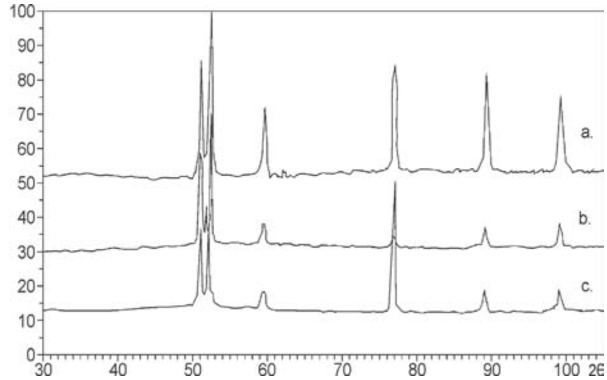


Fig. 44. Specification of diffraction patterns of welds of the samples: a - No. 1, b – No. 5, c – No.9 after grinding off the weld face to 2 mm depth, ferrite and austenite [4]

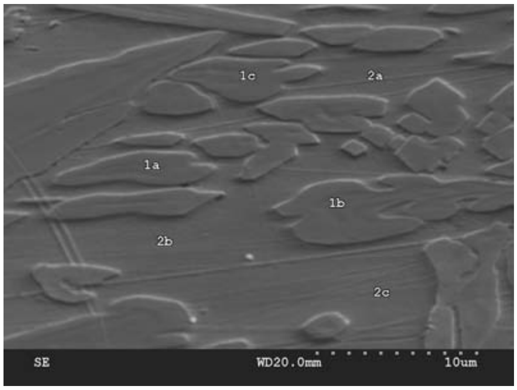


Fig. 45. Typical electron microscopy image of examined of the HAZ exemplified by specimen No. 9, root side, ferritic – austenitic structure, and average value of ferrite share 35%

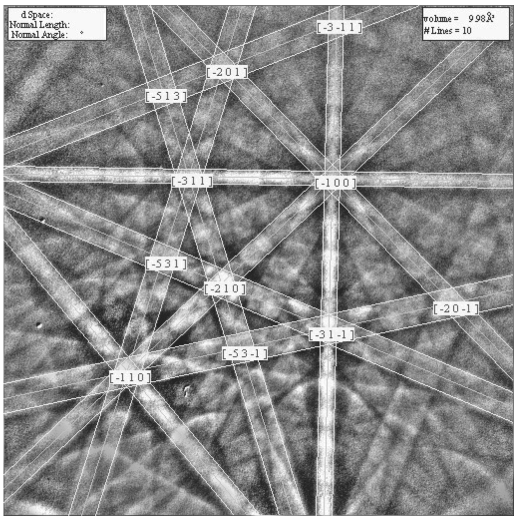


Fig. 46. Typical EBSD diffraction image of ferrite in the HAZ exemplified by specimen No. 9, root side

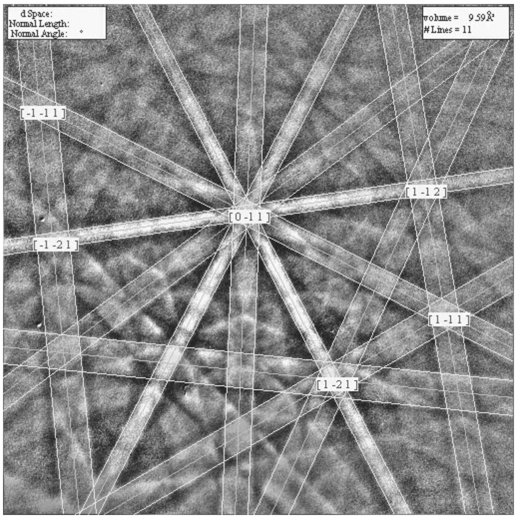

Fig. 47. Typical EBSD diffraction image of austenite in the HAZ exemplified by specimen No. 9, root side

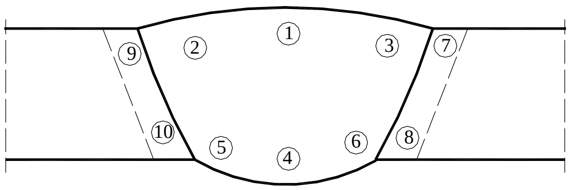


Fig. 48. Diagram of indents distribution in the HV10 hardness testing [4]

Table 21.
HV0.025 microhardness exemplified by sample No. 9 [4]

| Area on Fig. 48 | Ferrite | | | Austenite | | |
|---|---|---|---|---|---|---|
| | Test No. | | | Test No. | | |
| | 1 | 2 | 3 | 1 | 2 | 3 |
| 1 | 341 | 334 | 304 | 351 | 346 | 347 |
| 2 | 332 | 328 | 325 | 354 | 356 | 362 |
| 3 | 301 | 308 | 296 | 357 | 356 | 328 |
| 4 | 327 | 318 | 328 | 345 | 383 | 347 |
| 5 | 284 | 349 | 331 | 345 | 353 | 344 |
| 6 | 296 | 317 | 315 | 341 | 347 | 394 |
| 7 | 303 | 331 | 325 | 346 | 376 | 287 |
| 8 | 343 | 346 | 345 | 351 | 359 | 361 |
| 9 | 313 | 325 | 329 | 353 | 382 | 329 |
| 10 | 247 | 290 | 327 | 343 | 336 | 275 |

Table 22.
HV10 hardness exemplified by sample No. 9 [4]

| Area on Fig. 48 | Test No. | | |
|---|---|---|---|
| | 1 | 2 | 3 |
| 1 | 305 | 309 | 313 |
| 2 | 306 | 308 | 315 |
| 3 | 318 | 321 | 321 |
| 4 | 323 | 343 | 325 |
| 5 | 329 | 334 | 327 |
| 6 | 324 | 338 | 329 |
| 7 | 338 | 342 | 328 |
| 8 | 332 | 353 | 316 |
| 9 | 335 | 349 | 317 |
| 10 | 323 | 331 | 324 |

The corrosion resistance tests were performed according to ASTM G48 - 76 standard using method A.

The test pieces were collected from the welded joints mechanically (cut with bandsawing machine). Then they were subjected to grinding off treatment (using abrasive disks of granularity 120) and to polishing with polish disks. The test pieces, prior to undergoing corrosion resistance tests, were subjected to 2 hour passivation using the pickling and passivating paste - Avesta Pickling Paste-101.

The test solution was prepared from: ferric chloride (III) $FeCl_3{\cdot}6H_2O$ (100g) and distilled water (900 ml). The test pieces were immersed in test solution for 24 hours. After the performed tests visual examination of the test pieces surfaces and weighing were carried out.

In none of the examined test pieces corrosion pits were detected. The highest mass decrement (loss) equal to 3.5 mg (the permissible level being 20 mg) was found out on test piece No. 2. Negligible loss (decrement) in mass was observed in all test pieces with high corrosion resistance of the passive layer.

## 11. Conclusions

Development of applications of the duplex steel is distinct and concerns mainly welded constructions in the crude oil and gas extractive industry, chemical industry, petrochemical industry, shipbuilding industry, papermaking industry and pharmaceutical industry.

The fundamental question at welding the duplex steel is ensuring of the equilibrium of a relative volume of ferrite and austenite and non-allowing for processes of release the carbides and intermetallic phases causing decrease of the mechanical properties and corrosion resistance. The duplex steel crystallizes primarily as the ferritic one while transition of ferrite into austenite takes place in the solid state only. Too high cooling rate may slow down a process of transition ferrite into austenite what shall influence on the equilibrium of a relative volume of ferrite and austenite.

The value of welding heat input El. and inter-bead temperature is very important when welding the duplex steel in connection with their influence on the kinetics phase transitions and release processes and should be from 0.5 to 2.5 KJ/mm while inter-bead temperature should be in the range of 150-200°C.

Preheating is not used. The value of allowable welding heat input should be in each case subject to experimental verification.

Important question is the proper selection of additional materials for welding of the duplex steel, influencing on the relative volume of ferrite and austenite in a joint and, as a result, on the mechanical properties and corrosion resistance of a joint.

Shielding gases and gases used to shield a root of weld may control the nitrogen content in a joint and the relative volume of ferrite and austenite. Absence of nitrogen in a shielding gas may cause decrease of corrosion resistance of a joint, e.g. when welding with the TIG method.

High degree of difficulties of welding technology in case of large-size ship structures is caused by:

- low tolerance of deviations from the welding conditions required,
- considerable rigidity of long intersection joints prepared for welding in connection with moderate deposited metal ductility of the welding materials used,
- high requirements of site acceptance tests of joints welded.

Obtaining good mechanical properties and corrosion resistances is possible due to meticulous obeying the technological parameters of welding, minimization of assembly stresses in an area of joints welded as a result of observing assembly and welding sequence as well as taking into consideration the results of measurements of a structure geometry, automation and mechanization of welding processes stabilizing current parameters as well as detailed inspection on each production stage [22].

Increase of the welding heat input in submerged arc welding of duplex steel results in decrease of occurrence and size of welding imperfections with regard to a quantity and length of imperfections.

Increase of the welding heat input improves of the weld shape coefficient and decreases possibility of cracks creation. Mechanical tests of joints welded with maximal hit input HI $\leq$ 2.5; HI $\leq$ 3.0; HI $\leq$ 3.5; HI $\leq$ 4.0kJ/mm fulfilled requirements for duplex steel acc. to Det Norske Veritas Rulesand showed, that there was no negative influence of hit input increase on welds quality, in considered hit input range, on mechanical properties of joints.

As a result of the tests, it can be stated that increase of plate thickness increases weld defectiveness of duplex steel. Increase of welding hit input reduces occurrence of inadmissible welding imperfections in joints, what reduces costs of testing and repairs.

Based on the performed tests it was proved that the welding heat input exceeding the recommended values had no negative impact on strength properties and corrosion resistance of the executed welded joints, as:

- the obtained results of strength testing of butt-welded joints, with applied heat input ranging from 3 to 5 kJ/mm are at an acceptable level with considerable strength margin,
- the performed microstructure butt joints with butt weld examination at x 400 enlargement proved that there were no intermetalic and carbides phase release, including sigma phase,
- the performed microstructure tee joints with butt weld examination at x 400 magnification whereas at multiple-pass welding of joints with constant heat input applied in some test pieces appeared release of secondary austenite in the weld area,
- the corrosion resistance test of the test butt joints with butt weld yielded positive result without any corrosion pits, and the tested joints mass decrement is at a level 1.25 mg, according to guidelines of Det Norske Veritas and American Bureau of Shipping the specimen mass loss smaller than 20 mg is acceptable
- the performed corrosion resistance tests tee joints with butt weld did not show any corrosion traces (pits), whereas loss in mass was lower in 28 mm thick tested plate than in case of tested thinner plates using the same hat input of welding.
- average value of ferrite share, especially in heat affected zone (HAZ) of the welded joint was smaller than 70% level what in each of the variants complies with criteria specified both in the DNV rules, and in the references,
- welding of butt joints, using constant heat input, of both 9, 14 and 28 mm thick plates gives comparable values of ferrite share in the executed welded joints.

The weld and heat - affected zone structure consisted of primary ferrite grains with primary austenite precipitated on the grain boundaries, and with secondary austenite growing as a Widmanstätten type from the grain boundary austenite into the ferrite grains. Secondary austenite formed in the ferrite and at ferrite/austenite phase boundaries. Volume fraction of ferrite ($\alpha$) austenite ($\gamma$) and secondary austenite ($\gamma$2) are strongly influenced by welding.

Thermal the past of heat - affected zone has a substantial influence on its structure and properties. Precipitates of $\gamma$2 formed as a result of post weld aging have a most important influence on HAZ hardness.

Pitting corrosion resistance of the welds is strongly influenced by thermal cycle parameters. A different level of Chromium and nickel constitution in the $\alpha$, $\gamma$ and $\gamma$2 phases, as well as a phase volume fraction have a significant influence on corrosion resistance. Generally post weld heat treatment decreases the pitting corrosion resistance.

Primary austenite has a bigger hardness compared with ferrite for the every post weld conditions. The secondary austenite hardness is influenced by chemical composition changes of the phase.

The presence of the intermediate phases, carbides, and nitrides precipitates in a heat-affected zone of a welded joint of duplex steels was not observed.

The performed tests and examinations of welded joints with root face gap ranging from 6 to 10 mm were intended for extending the standard range from 2 to 6 mm. Thus increased range is optimum, considering assembly and welding of large-size constructions where the technology permits for example cutting off the assembly allowances. Increase of the root face gap above 10 mm unjustified economically and it may cause considerable deformations of welded constructions.

The performed non-destructive testing indicate the possibility to obtain welded joints of the required high quality, even in case of welded test pieces with the root face gap 10 mm. As a result of the performed inspection, decreasing of the ferrite content (share) with the increase of the root face gap (increase of welding heat input) was observed. The minimum measured ferrite content (share) was not lower than 28 % and the maximum value did not exceed 69% (the permissible range being from 25 to 70 %).

The structural tests and examinations carried out confirm occurrence of only two phases: that of austenite and that of ferrite. In none of the tested and examined areas occurrence of micro-cracks, intermettalic phases or releases was detected.

Corrosion resistance tests performed with three methods indicate occurrence of the passive layer on the examined test pieces, characterized by considerable resistance to aggressive factors exposure.

Results of visual examinations of welded joints indicate necessity to change the construction of ceramic backings in case of welding with gaps exceeding 8 mm (increasing of the ceramic backing width and groove shape). Use of commonly available ceramic backings (like those used during the conducted tests of welding of PS-11/1.9 type backing made by IMO Gliwice) involves necessity of removal of undercutting of the root run occurring in the weld on both sides.

So as to sum up, one can conclude that the wide-gap welding (with root face gap up to 10 mm) of duplex steel joints in vertical position does not have an adverse effect on structural and corrosion-resistance properties.

When the technological process is carried out in an appropriate way, the welded construction can be executed (without the necessity to repair the welded joints geometry) using the extended range of the root face gap.

## References


[1] J. Adamczyk, Engineering of steel's products, Silesian University of Technology Press, Gliwice, 2000 (in Polish).

[2] J. Nowacki, P. Rybicki, Welding imperfections of submerged arc welded duplex steel joints in aspects of the welding heat input, Proceedings of the 11th International Scientific Conference "Contemporary Achievements in Mechanics, Manufacturing and Materials Science" CAM3S'2005, Gliwice − Wisła, 2005, (CD-ROM).

[3] J. Nowacki, P. Rybicki, Influence of heat input on corrosion resistance of SAW welded duplex joints, Journal of Achievements in Materials and Manufacturing Engineering 17 (2006) 113-116.

[4] J. Nowacki, P. Zając, Microstructure and corrosion resistance of the duplex steel wide-gap one-side fluxcored welded joints, Journal of Achievements in Materials and Manufacturing Engineering 29/2 (2008) 191-198.

[5] L.A. Dobrzański, Descriptive metal science of iron alloys, Silesian University of Technology Press, Gliwice, 2007 (in Polish).

[6] S. Atamert, J.E. King, Super duplex stainless steels. Part 1 Heat affected zone microstructures, Materials Science and Technology 8 (1992) 896-911.

[7] Avesta Polarit Welding – Catalogue, 2002.

[8] C. Messner, V.V. Silberschmidt, E.A. Werner, Thermally induced surface roughness in austenitic-ferritic duplex stainless steels, Acta Materialia 51 (2003) 1525-1531.

[9] M. Cholewa, J. Gawroński, M. Przybył, Fundamentals of metallurgical processes, Silesian University of Technology Press, Gliwice, 2004.

[10] Welding duplex stainless steels the ESAB way, Catalogue, ESAB, 2000.

[11] L. Karlsson, L. Ryen, S. Pak, Precipitation of intermetallic phases in 22% Cr duplex stainless weld metals. The kinetics of intermetallic phase formation in the temperature range 675-1000°C (1274-1832°F) and effects on mechanical properties and corrosion resistance, Welding Research Supplement (1995) 28-40.

[12] S. Czyżowicz, Corrosion resistance of new austenite-ferrite stainless steels, Works of IMŻ Gliwice 1-2 (1990) 35 (in Polish).

[13] J.D. Kordatos, G. Fourlaris, G. Papadimitriou, The effect of cooling rate on the mechanical and corrosion properties of SAF 2205 (UNS 31803) duplex stainless steel welds, Scripta Materialia 44 (2001) 401-404.

[14] J. Łabanowski, Effect of microstructure on mechanical properties of duplex stainless steel for marine applications, Marine Technology Transactions 10 (1999) 213-217.

[15] J. Łabanowski, K. Krzysztofowicz, A. Ossowska, Stress corrosion cracking of simulated heat affected zones of duplex steels welded joints, Materials Engineering 6 (2003) 731-736 (in Polish).

[16] Polish Standart PN-EN 10088-1,1998, Stainless steels (in Polish).

[17] R. Abdel-Karim, I. Elmahallawi, K. El-Menshawy, Microstructure and corrosion properties of nitrogen stainless steel 316L produced by hipping, Powder Metallurgy 47/1 (2004) 43-48.

[18] J. Banas, A. Mazurkiewicz, The effect of copper on passivity and corrosion behaviour of ferritic and ferritic-austenitic stainless steels, Materials Science and Engineering A 277 (2000) 183-188.

[19] X.-C. Lu, K. Shi, S.-Z. Li, X.-X. Jiang, Effects of surface deformation on corrosive wear of stainless steel in sulfuric acid solution, Wear 225-229 (1999) 537-541.

[20] J. Charles, Composition and properties of duplex stainless steels, Welding in the World 36 (1995) 43-47.

[21] W. Przetakiewicz, R. Tomczak, Some aspects of duplex and superduples ferrite-austenite steels wetability, Welding Technology Review 3 (1995) 1-7 (in Polish).
[22] J. Nowacki, M. Urbański, P. Zając, Welding of FCAW duplex steels in chemical transport ships construction, Welding Technology Review 4 (2008) 3-10 (in Polish).
[23] J.A. Jimenez, M. Carsi, O.A. Ruano, F. Penalba, Characterization of a δ/γ duplex stainless steel, Journal of Materials Science 35 (2000) 907-911.
[24] J. Nowacki, A. Łukojć, Microstructure transformations of duplex steels welded joints heat affected zone, Materials Characterization 56 (2006) 436-441.